UNIVERZA V LJUBLJANI
FAKULTETA ZA FARMACIJO

RENATA BOBNAR KAMNIKAR

MAGISTRSKA NALOGA

ENOVITI MAGISTRSKI ŠTUDIJ FARMACIJA

Ljubljana, 2014

UNIVERZA V LJUBLJANI

FAKULTETA ZA FARMACIJO

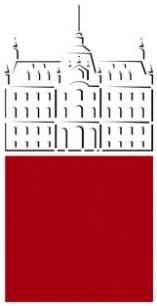

RENATA BOBNAR KAMNIKAR

LIPOSOMI S KVERCETINOM:

PRIPRAVA, VREDNOTENJE IN *IN VITRO* TRANSDERMALNA ŠTUDIJA

LIPOSOMES WITH QUERCETIN:

PREPARATION, EVALUATION AND *IN VITRO* TRANSDERMAL STUDY

Ljubljana, 2014

Raziskovalno delo za magistrsko nalogo sem opravila na University of Cagliari, Dipartimento di Scienze della Vita e dell'Ambiente, v sodelovanju s Fakulteto za farmacijo, Univerze v Ljubljani, pod somentorstvom prof. dr. Anne Maria Fadda in mentorstvom prof. dr. Julijane Kristl.

Zahvale

To delo ne bi moglo nastati brez pomoči nekaterih izjemnih ljudi, ki bi se jim ob tej priložnosti rada iskreno zahvalila.

Rada bi se zahvalila somentorici prof. dr. Anni Marii Fadda, ki mi je dala možnost, da sem bila del njene ekipe. Hvala za motivacijo in pomoč tekom dela na Univerzi v Cagliariju.

Prav tako se želim zahvaliti dr. Carli Caddeo za vodenje in podporo, ki mi jo je nudila. Magistrske naloge ne bi mogla izdelati brez HPLC meritev ter cryo-TEM posnetkov. HPLC analizo je izvedla dr. Donatella Valenti, docentka v raziskovalni skupini na Univerzi v Cagliariju, cryoTEM posnetke pa je pripravil Xavier Fernàndez-Busquets iz Nanobioengineering Group, Institute for Bioengineering of Catalonia, Barcelona.

Globoko sem hvaležna prof. dr. Julijani Kristl, da je sprejela vlogo mentorice, in mi je nudila strokovno vodstvo ter podporo pri pisanju magistrske naloge. Cenim njeno motivacijo in nasvete, prav tako pa tudi dejstvo, da mi je bila vedno pripravljena pomagati in me spodbujati.

Nenazadnje pa bi se rada zahvalila moji družini. Vesna, Silva in Dušan, hvala vam za vso ljubezen, podporo in potrpežljivost tako tekom študija kot med pisanjem magistrske naloge. Ob meni pa so bile vedno tudi Barbara, Diana, Helena, Metka in Nina – hvala vam za pomoč, podporo in vse lepe spomine v času študijskih letih.

Izjava

Izjavljam, da sem diplomsko nalogo izdelala samostojno pod mentorstvom prof. dr. Julijane Kristl in somentorstvom prof. dr. Anne Marie Fadda.
Ljubljana, januarja 2014

Podpis študentke: Renata Bobnar Kamnikar

Člana komisije:

Predsednik diplomske komisije: prof. dr. Aleš Mrhar
Član diplomske komisije: doc. dr. Matej Sova

The present master thesis was realized at University of Cagliari, Dipartimento di Scienze della Vita e dell'Ambiente, with collaboration of the Faculty of Pharmacy, University of Ljubljana. I worked under the host supervision of Prof. Dr. Anna Maria Fadda and home supervision of Prof. Dr. Julijana Kristl.

Acknowledgments

This work could not have been realized without the help of some extraordinary people and I would like to express my sincere gratitude at this point.

I would like to thank my host supervisor, Prof. Dr. Anna Maria Fadda, for giving me the opportunity to be a part of her team, her motivation and help throughout my work at the University of Cagliari.

I also wish to thank Dr. Carla Caddeo for all the instructions, guidance and support she gave me. Moreover, it wouldn't be possible to finish my work without HPLC analyses and cryo-TEM observations. HLPC analyses were carried out by Dr. Donatella Valenti, assistant professor of the research team at the University of Cagliari, Italy, and cryoTEM was carried out by Xavier Fernàndez-Busquets from Nanobioengineering Group at Institute for Bioengineering of Catalonia, Barcelona, Spain.

I am grateful to Prof. Dr. Julijana Kristl, for being my home supervisor, who offered me professional leadership and support. I appreciate her assistance, motivation and advices. She was always willing to help me and encouraged me to do my best.

Finally, I would like to thank my family. Their love, support and patience helped me to complete this work. And thank you, Barbara, Diana, Helena, Metka and Nina, for help, support and all the nice memories during study years.

Statement

Hereby, I testify having performed the experiments to the best of my knowledge and having written this thesis independently under the guidance of my supervisors:
Prof. Dr. Anna Maria Fadda and Prof. Dr. Julijana Kristl
Ljubljana, January 2014

Student signature: Renata Bobnar Kamnikar

President of the Thesis defense committee: Prof. Dr. Aleš Mrhar
Member of the Thesis defense committee: Assist. Prof. Dr. Matej Sova

Table of Contents

Povzetek

Dermalno dajanje kvercetina bi lahko zagotovilo neposredno zaščito kože pred škodljivim delovanjem sončnih žarkov in lokalno zdravljenje različnih kožnih bolezni. Sam kvercetin kot tak zaradi slabe topnosti v vodnem okolju in slabe prehodnosti skozi kožo ni primeren za dermalno dajanje. V magistrski nalogi smo se posvetili izboljšanju dermalne dostave kvercetina in sicer z vgradnjo kvercetina v izdelane inovativne vezikle.

Cilj projekta je bil izboljšati vgradnjo kvercetina v liposome ter prodiranje in dostavo v kožo. Za dosego le-tega smo zasnovali liposome z uporabo ene izmed dveh fosfolipidnih mešanic (Lipoid S 75 in Phospholipon® 85 G) in penetracijskih pospeševalcev (PEG 400 in oleinska kislina). Liposome pripravljene s sonikacijo smo fizikalno ovrednotili (povprečna velikost, njena distribucija, zeta potencial) z metodo dinamičnega sipanja laserske svetlobe. Učinkovitost vgrajevanja kvercetina v liposome smo določili s HPLC analizo, morfološke značilnosti izdelanih liposomov pa smo pridobili z zmrzovalno presevno elektronsko mikroskopijo. Uspešnost združevanja lipidov v liposomskih disperzijah smo ocenili spektrofotometrično s Stewartovim testom. Po pregledu rezultatov smo izbrali vzorce za *in vitro* študijo dermalne penetracije. Z uporabo statične Franz-ove difuzijske celice smo določili možnost penetracije v kožo CD-1 miši za liposome s PEG (PEG-PEVe), kontrolne liposome ter PEG-disperzijo.

Pripravljeni liposomi s PEG so bili stabilni, medtem ko so tisti z oleinsko kislino (OA) v različnih koncentracijah izkazovali veliko nestabilnost, prav tako tudi liposomi pripravljeni z obema pospeševalcema penetracije PEG-OA-PEVi, zato jih v *in vitro* študijah nismo uporabili. Rezultati, ki smo jih pridobili tekom raziskave, kažejo na visoko vgrajevanje kvercetina (52-75%) v izdelanih liposomih s PEG 400. Z *in vitro* študijo smo dokazali, da se je kvercetin v plasteh kože akumuliral v manj kot 1%. PEG v vzorcih PEG-PEV in v PEG disperziji ni statistično izboljšal pospeševanja penetracije in akumulacije med kontrolnimi liposomi ($p>0.05$). Vse formulacije so vodile k permeaciji skozi kožo in sicer je bila vsebnost kvercetina v receptorskem mediju do 0.4%.

Ključne beside: kvercetin, liposomi, polietilenglikol 400, pospeševalci penetracije, koža.

Abstract

Dermal application of quercetin (QUE) might provide direct skin protection and local therapy of various skin diseases. QUE as such is inappropriate for dermal application due to poor solubility in aqueous media and low skin permeability. The aim of master thesis was devoted to improve QUE dermal delivery by QUE entrapment into the developed innovative vesicles.

The aim of the project was to improve entrapment efficiency of QUE in liposomes and skin penetration and dermal drug delivery of QUE, therefore liposomes using different phospholipid mixtures (Lipoid S 75 and Phospholipon® 85 G) and penetration enhancers (PEG 400 in oleic acid) were designed specifically to improve QUE incorporation in liposomes and promote transdermal permeability. Liposomes with various compositions were prepared by sonication and characterized by different methods. In particular, liposome morphology was determined and the main physico-chemical features (size, its distribution and zeta potential) were assessed by light scattering. Afterwards, drug loading efficiency was determined by HPLC and the Stewart assay was used to spectrophotometrically determine the lipid content in the liposome dispersions. Subsequently, *in vitro* dermal penetration studies using Franz diffusion vertical cells were carried out. Full-thickness CD-1 mouse skin was used to evaluate penetration capability of QUE-loaded PEG-PEVs, control liposomes and PEG dispersion.

Liposomes designed with PEG were stable, liposomes with oleic acid have shown low stability and were not used in transdermal studies, and PEG-OA-PEVs sample as well. Results showed high entrapment efficiency (52-75%) of QUE in prepared PEG-PEVs. The amount of QUE accumulated in skin layers was less than 1% with all of the samples and no statistically significant enhancement of accumulation was demonstrated among the control liposomes, PEG-PEVs and PEG dispersion after the *in vitro* transdermal study ($p>0.05$). However, all the studied formulation led to a transdermal QUE delivery, but the drug delivery to the receptor fluid was very low (up to 0.4%).

Keywords: quercetin, liposomes, polyethylene glycol 400, penetration enhancer, skin.

Abbreviations

AE% – aggregation efficiency

EE% – entrapment efficiency

GSH – glutathione

HPLC – high performance liquid chromatography

MD – mean diameter

OA – oleic acid

PBS – phosphate buffer solution pH 7.4

PCS – photon correlation spectroscopy

PE – penetration enhancer

PEG – polyethylene glycol 400

PEVs – penetration enhancer-containing vesicles

PI – polydispersity index

QUE – quercetin

ROS – reactive oxygen species

Cryo-TEM – cryogenic-transmission electron microscopy

ZP – zeta potential

1 Introduction

There is a growing focus on the use of naturally profuse compounds as dietary supplements over the past decades. A range of dietary flavonoids have become point of interest along with the awareness that also traditional folk medicines still in use around the world contain flavonoids. Consequently, numerous studies have been carried out in order to determine biochemical and physiological activities of flavonoids and to explain health benefits related with fruit- and vegetable-rich diets.

1.1 Flavonoids

Flavonoids occur naturally in the plant kingdom and are widespread in edible fruits and vegetables. More than 5000 polyphenolic members have been identified to date (1). They are responsible for pigmentation and for normal growth and defense of plants and are also an important integral part of the human diet, since they can be found in vegetables, fruits, and also in some beverages such as red wine, tea and coffee (2). Flavonoid intakes of individuals for several countries have been calculated. According to Beecher, total daily flavonoids intake ranges from approximately 20 mg in United States, Denmark and Finland to more than 70 mg in Holland. However, earlier estimates (from several hundred mg/d to 1g/d) were much lower compared to these values and there is a great discrepancy of consumption data. Consequently, the lack of extensive food composition data for flavonoid subclasses does not allow their precise daily intake determination (3).

Flavonoids are categorized into seven subclasses: anthocyanidins, flavan-3-ols, flavanones, flavanonols, flavones, flavonols and isoflavones. Their structures are schematically depicted in Fig. 1. The division into classes is based on the connection of the B ring to the C ring and on the oxidation state and functional groups of the C ring (3). Table I lists the subclasses of flavonoids in alphabetical order with members of each subclass, some common food sources, and estimated daily intakes. There are a large number of molecules identified within each flavonoid subclass, since most flavonoids are present in nature as both simple or complex glycosides and other conjugates (1).

Table I: Common dietary flavonoids (3-6)

Flavonoid Subclass	**B-ring connection to C ring (position on C ring)**	**Dietary flavonoid**	**Common food sources**	**Estimated daily intakes (mg/d)**
Anthocyanidins	2	Cyanidin Delphinidin Malvidin Pelargonidin Peonidin Petunidin	Red, blue, and purple berries, red and purple grapes, red wine	3.1
Flavan-3-ols	2	Monomers (Catechins): Catechin Epicatechin Epigallocatechin Epicatechin gallate Epigallocatechin gallate Dimers and Polymers: Theaflavins Thearubigins Proanthocyanidins	Catechins: Teas (particularly green and white), chocolate, berries grapes, apples Theaflavins, Thearubigins: Teas (black and oolong in particular) Proanthocyanidins: Chocolate, apples, berries, red grapes and wine	156.9
Flavanones	2	Eriodictyol Hesperetin Naringenin	Citrus fruits and juices	14.4
Flavanonol	2	Taxifolin (Dihydroquercetin) Dihydrokaempferol	Citrus fruits	/
Flavones	2	Apigenin Luteolin	Green leafy spices, e.g., Parsley	1.6
Flavonols	2	Isorhamnetin Kaempferol Myricetin Quercetin	Widely distributed: yellow onions, kale, broccoli, apples, berries, teas	12.9
Isoflavones	3	Daidzein Genistein Glycitein Biochanin A Formononentin	Soybeans, soy foods and legumes	1.2 (US and Netherlands) 25 – 50 (Asia)

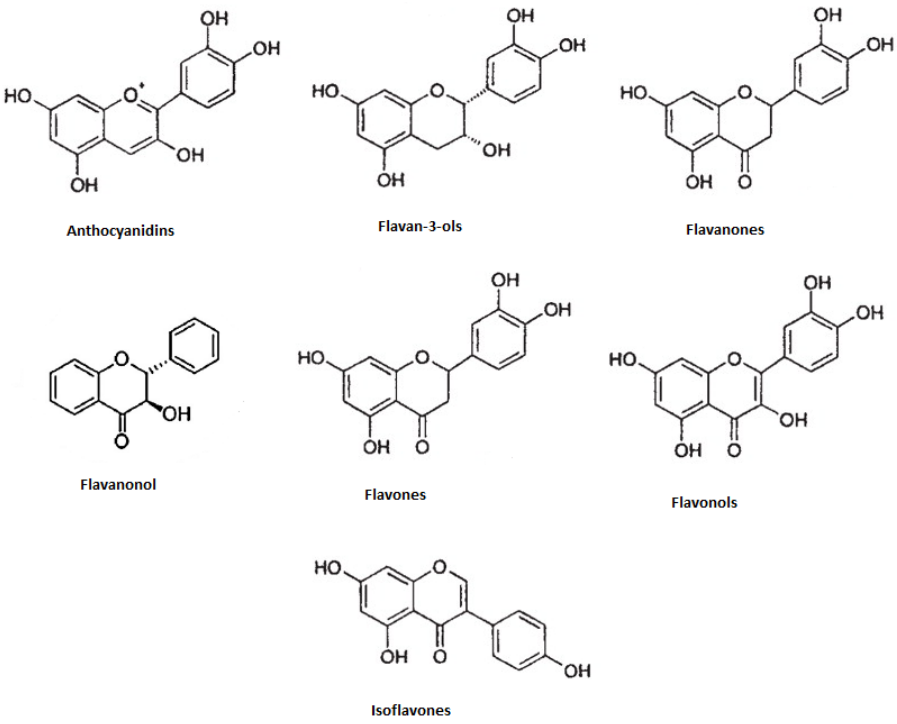

Figure 1: Structures of flavonoid subclasses (6, 7)

1.2 Quercetin

The most commonly investigated member of the flavonoid family is quercetin (3,3',4',5,7-pentahydroxyflavone, QUE, Fig. 2), which is one of the most prominent dietary antioxidants. QUE presents the highest antiradical property compared to other flavonoids (8) and is the most potent scavenger of reactive oxygen species (ROS), including $O_2^{\bullet -}$, and reactive nitrogen species (RNS) like $NO^{\bullet}$ and ONOO− (9).

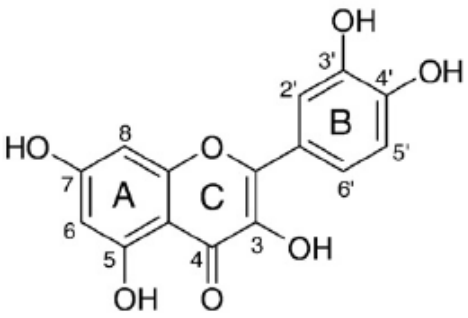

Figure 2: Quercetin chemical structure

1.2.1 Antioxidant activity

The existence of two antioxidant pharmacophores in the QUE molecule is the reason for its excellent *in vitro* antioxidative abilities. OH group at position 3 of the AC ring and catechol group in the B ring have the optimal configuration to scavenge free radicals. Furthermore, it has been proposed that QUE with its contribution to the total plasma antioxidant capacity significantly enable the endogenous antioxidant shield. Compared to the reference antioxidant trolox, QUE's contribution is 6.24 times higher, while the contribution of vitamin C and uric acid together approximately match that of trolox (9).

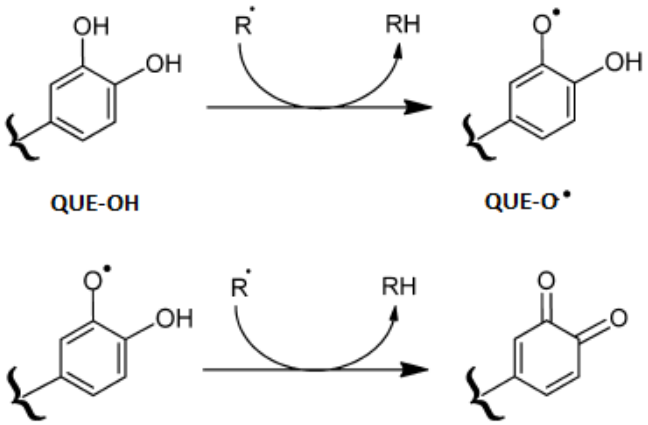

Figure 3: Scavenging of ROS ($R^{\bullet}$) by quercetin. The free radical QUE-$O^{\bullet}$ may react with another radical acquiring a stable quinine structure (7).

1.2.2 Pharmacological activity

In addition to antioxidant activity, QUE possesses a wide range of biological activities and pharmacological actions. Anti-cancer, anti-inflammatory, decreasing blood lipid levels, dilating coronary arteries, anti-platelet aggregation, anti-anemic and anti-anaphylaxis effects are just some of these (10). Principal mechanisms that lead to the protective effects of the drug have been asigned to the inhibition of key signaling enzymes like protein kinase C, tyrosine kinase and phosphoinositide 3-kinase. They regulate cell proliferation, angiogenesis and apoptosis. Another important property that significantly brings to the protective outcome is previously mentioned scavenging of ROS (11). It has been shown

that ROS generation by QUE increased apoptotic cell death and apoptosis signal-regulating kinase-1 (ASK1) activation occurred. QUE was suggested to implement apoptotic effects through ROS/AMPKa1/ASK1/p38 signaling pathway, while AMP-activated protein kinase (AMPKa1) is necessary for apoptosis (12). Moreover, inhibition of Na^+K^+ATPase, HIV reverse transcriptase, Ca^{2+}-ATPase of sarcoplasmic reticulum, and $pp60^{src}$ kinase was demonstrated. QUE is reported to cause cell cycle arrest of human leukemic T cells and gastric cancer cells in late G1. Besides that, antiproliferative activity *in vitro* against breast, ovarian, and stomach cancer cell lines was shown (13).

1.2.3 Anti-inflammatory properties

Another strong capacity of QUE is the anti-inflammatory one. Numerous *in vitro* studies using different cell lines have revealed that QUE can inhibit LPS-induced cytokine production. Furthermore, it has been shown that the flavonoid can inhibit LPS-induced TNFα production in macrophages and IL-8 production in lung cells and mRNA levels of TNFα and IL-1α in glial cells (14-16). ROS are involved in the occurrence of oxidative stress as well as in promoting inflammatory processes by activating transcription factors that are responsible for induction of cytokine production (e.g. TNFα) (17). Given that, this may represent a reasonable clarification for QUE anti-inflammatory properties. In fact, it has been proven that QUE can inhibit both the production of gene and gene expression of TNFα through modulation of NF-κB (18).

1.2.4 Actions on skin

More recently, it has been noticed that QUE can reduce the expression of matrix metalloproteinase-1, which is responsible for loss of elasticity and consequently for skin wrinkling. This is possible at protein as well as mRNA levels (19). Moreover, after dermal application of QUE to the skin, potent inhibition of UVB-induced oxidative skin damage occurs (20). Evidence of two clinical trials, where QUE considerably reduced contact dermatitis and photosensitivity, can be found in literature. These two skin conditions are difficult to manage and often also don’t respond to conventional treatment (21). In addition, it has been proven that QUE owns also antibacterial activity against bacteria that cause skin disorders (22). External factors and toxins are origin to oxidative stress in skin, and given that QUE can effectively protect the skin from these agents, dermal application

of the flavonoid has received considerable attention. Furthermore, QUE is considered a promising candidate to treat also allergic and inflammatory diseases.

1.2.5 Quercetin paradox and genotoxicity

On the whole, studies specify that QUE can apply health-beneficial capabilities through a variety of damage modulating effects. QUE has natural origins and good safety profile. This makes it an attractive candidate for different formulations. However, there are some drawbacks that might be considered. Firstly, when participating in oxidative actions, QUE becomes oxidized into various oxidation products. The resulting quercetin-quinone (QQ) has four tautomeric forms, i.e. an orthoquinone and three quinonemethides. It is well known that semiquinone radicals and quinones exhibit a range of toxic effects resulting from their capacity to arylate protein thiols. QQ is very reactive towards thiols and can immediately form adduct with glutathione (GSH), which is the most abundant of endogenous thiols and appears to be the most important reactant of QQ. The adduct that is formed (GSQ) is not stable; the half life for dissociation into GSH and QQ is 2 minutes. It has been shown that GSH traps QQ as GSQ until concentration of GSH is high enough. When its concentration decreases, the dissociated QQ can react with other thiol groups, e.g. protein sulfhydryls. This may indicate that the "protection" that submits GSH against QQ might only be momentary. GSH can protect against QQ at the time and site of formation, but eventually quinine will be transferred to other thiols. Consequently, toxic effects can occur. Increase in membrane permeability and alternations in enzymes' activity that include SH-group, are one of them. This QQ-induced toxicity has been shown in several *in vitro* studies. It has been defined as the quercetin paradox, i.e. the conversion of QUE into a potential toxic product while offering protection by scavenging ROS (9). However, the *in vivo* formation of QQ and its possible toxicity has not been displayed yet. Secondly, it has also been demonstrated that QUE demonstrates genotoxic effects *in vitro*. Mutagenic effects are above all presented in bacteria and quinone formation has been suggested to be necessary (23). However, reported data concerning the QUE ability to induce DNA lesions and mutations in mammalian cells and experimental animal are contradictory. More research has to be carried out in order to clarify the potential genotoxic effects of QUE to human body.

1.2.6 Poor water solubility

Other difficulties regarding QUE are its physical properties. It has low solubility and consequently low absorption *in vivo*. Solubility in water has been reported to be 7.7 μg/mL, in simulated gastric fluid 5.5 μg/mL and in simulated intestinal fluid 28.9 μg/mL (24). For example, no measurable plasma concentration has been reported in human volunteers from a 4 g oral dose. Minimal absorption from the gastrointestinal tract is a result of extensive metabolism by the gut microorganisms (25). Data for an octanol–water partition coefficient (log P) are not consistent. LogP for QUE according to Rothwell et al is 1.82±0.32 (26) and as reported by Lin et al is 3.38±0.03 (22). A latter study investigated relationships of the structure and activity with skin permeation. For the purpose of the study, the lipophilicity of QUE, its aglycone, a polymethoxylated compound (quercetin 3,5,7,30,40-pentamethylether, QM), and seven glycosides was defined and graded by log K'. Log K' illustrate the relative retention of the HPLC system. QUE showed the second highest log K' (0.97), right after the value of QM (1.67) (22). As regards the log P of QUE, is theoretically satisfactory to permeate the skin. On the other hand, bioavailability is believed to be limited by restricted solubility in water that hinders permeation through the skin (27). In addition, the physical barrier in skin is mainly localized in stratum corneum (SC), which is the outermost skin layer. It consists of protein-enriched dead cells and lipid-enriched intercellular domains (28). In the experiment of Lin et al, the stratum corneum was stripped in order to investigate its role on the absorption of QUE and the derivates. It was found out that this act enhanced flux of each compound, including QUE, whose flux through stripped skin was 4.14-times greater than the one through intact skin (22).

1.3 Advantages of dermal application of QUE

Bearing in mind that the extension of the beneficial effects of QUE observed in *in vitro* studies to the *in vivo* studies or clinical level with an oral delivery approach is greatly restricted, skin delivery may present an attractive alternative. Transdermal drug delivery is defined as an administration of a therapeutic agent through intact skin to obtain systemic effect, while percutaneous delivery is transport into target tissues with an attempt to avoid systemic effects (29). Success of the approach to use drug for systemic drug delivery depends on the capacity of the drug to permeate into and penetrate through skin. In order to

achieve desired therapeutic effect, drug has to penetrate through the skin in sufficient quantities (30). Several advantages can be observed when comparing transdermal drug delivery with the oral route for controlled drug delivery. We can avoid gastrointestinal absorption and hepatic first pass metabolism and there is no interference with gastric and intestinal fluids. Moreover, we are able to moderate the characteristics of the biological barrier, administrate drugs with poor oral bioavailability, and terminate the drug administration with removing the application. Finally, another important aspect is improvement of patient compliance and comfort with simple, non-invasive and painless application (30-32). However, there are also some disadvantages of transdermal drug delivery approach. Many drugs with a hydrophilic structure have a low penetration through the skin and some drugs' molecular sizes make absorption difficult (ideal below 800-1000 Daltons). It is important bearing in mind that the barrier function of the skin alters from person to person as well from one site to another on the same person and depends on age. It has to be stated that high drug levels in blood/plasma cannot be achieved by transdermal drug delivery (32). On the other hand, dermal application of QUE might provide direct targeting to achieve skin protection and local therapy of various skin diseases and conditions. Therefore, the development of novel vesicles that are able to incorporate QUE and to transport it into the skin is needed.

1.4. Skin composition and transdermal permeation

Skin is the largest organ of the human body; its surface area covers approximately two square meters and receives about one third of the blood circulating through the body (32). Its main functions are protection of major or vital internal organs from the external chemical, physical and microbiological influences, temperature regulation, sensation and maintenance of electrolyte and fluid balance. Moreover is skin capable of synthesis, processing and metabolism of structural proteins, glycans, lipids, and signaling molecules. It's becoming more and more clear that the skin represents an integral component of the endocrine, nervous and immune system (33). Since skin is outermost protective shield against the harmful environmental agents and is directly exposed to external factors, like ultraviolet and ionizing radiation, ozone, and toxic chemicals, it must be a good permeability barrier. It is made up of numerous anatomically distinct layers: the non-viable stratum corneum and the viable epidermis and the dermis to form the main physical barrier

in skin. The main constituents are keratin-filled dead cells called corneocytes. They are completely surrounded by crystalline lamellar lipid regions. Over most of the body, 10 to 20 cell layers build up the stratum corneum. Each cell is a flat, plate-like structure - 34-44 μm long, 25- 36 μm wide and 0.5 to 0.20 μm thick. Skin barrier function depends on its total architecture, which has been described as the 'bricks and mortar' model where the bricks are the corneocytes and the mortar refers to the lipid rich matrix (30, 34).

Molecules applied to skin surface penetrate and permeate through the barrier by a passive diffusion process. There are two possible diffusion routes: the transappendageal and the transepidermal. The first route includes transport via the sweat glands and hair follicles, including their sebaceous glands. Although traditionally considered of minor importance, recent research has indicated that the pilosebaceous units may contribute significantly to topical drug delivery by providing a low resistance pathway for large polar molecules and ions that barely permeate through the stratum corneum. The transepidermal route consists of transcellular (through the corneocytes) and intercellular pathway (across the lipid domains between the corneocytes). The intercellular route is generally accepted as a principal pathway for the permeation of most drugs (28).

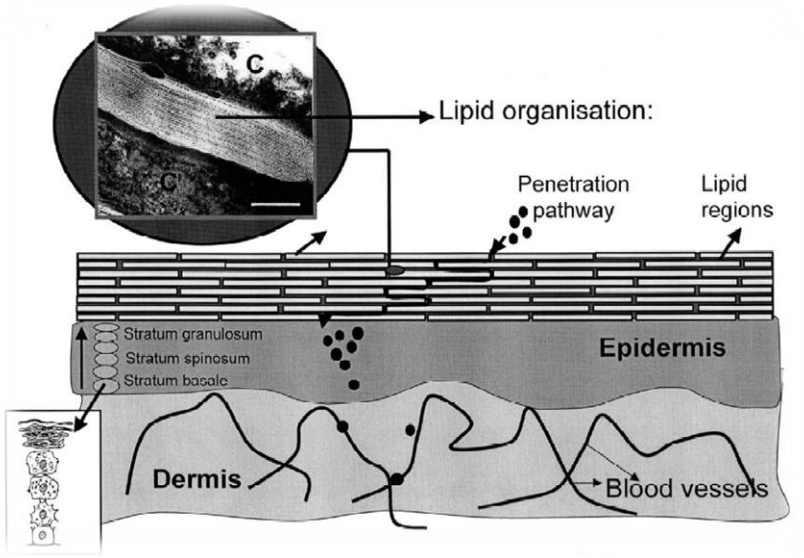

Figure 4: A skin cross-section. The stratum corneum with 10-20 cell layers, epidermis and dermis. Cells proliferate in the basal layer of epidermis. As a result of leaving the basal layer cells start to differentiate and migrate in the direction of the skin surface. Final differentiation occurs at the interface between stratum granulosum and stratum corneum, where the viable cells are transformed into dead keratin filled cells (corneocytes) (30).

1.5. Skin penetration enhancers

In order to be successful in dermal and transdermal delivery, efficient penetration of active compounds through the skin barrier must be ensured. Additionally, transdermal delivery requires efficient permeation through the skin. Different permeability can be achieved through various approaches and attempts to lower the skin permeability barrier have been several. They vary from drug and vesicle interactions, various vesicles and particles, change and removal of stratum corneum to electrically assisted methods and others (35).

Penetration enhancers (PE) are defined as substances that facilitate the drug penetration through the skin. This happens by temporarily decreasing the skin impermeability. Ideally, these materials should be pharmacologically inert, nontoxic, non-irritating, non-allergenic, compatible with the drug and excipients, odorless, tasteless, colorless, and inexpensive and have good solvent properties. The loss of body fluids, electrolytes, and other endogenous compounds should not be a result of using PE and skin should renovate its barrier characteristics and functions right away (36). Mechanisms of chemical penetration enhancement include disruption of the highly ordered structure of the stratum corneum lipids, interaction with intercellular proteins and improvement of penetration of the drug, coenhancer or solvent into the stratum corneum (30).

In the literature can be found different enhancers, such as water, sulfoxides (especially dimethylsulfoxide) and their analogues, pyrrolidones, fatty acids, esters and alcohols, anionic, cationic and nonionic surfactants, amides with urea and its derivatives, polyols, essential oils, terpenes and derivatives, oxazolidines, epidermal enzymes, polymers, lipid synthesis inhibitors, biodegradable enhancers and their synergistic mixtures. Water is believed to be the best penetration enhancer in terms of safety and effectiveness (35). When hydrating stratum corneum, the penetration rate of most substances increases, because water opens up the compact structure of horny layer (37). Yet, it has been demonstrated *in vivo* that elevated hydration may not always expand drug permeation (38).

1.6. Colloidal carrier vesicles

Much data have been reported on specially designed vesicular carriers that can be used to expand systemic delivery but also to localize the drug in skin layers for local treatment of various skin disorders. Vesicular carriers can be divided into two main classes: liposomes (vesicles mostly made up of phospholipids, discovered by Bangham in 1960) and non-ionic surfactant vesicles (discovered by L'Oreal in the 1970s and called niosomes) (28). Gregoriadis et al defined liposomes as spherical vesicles composed of one or more phospholipid bilayers. Generally, phospholipid bilayers consist of phosphatidylcholine, where lipophilic drugs can be incorporated. On the other hand, solubilization of hydrophilic drugs in the inner aqueous core is possible (39). Drug release, biodistribution and *in vivo* stability are influenced by vesicle size and surface charge, surface hydrophobicity and membrane fluidity (40). Moreover, appropriate selection of phospholipids composition and additives also modify the membrane permeability.

In this work we studied penetration enhancer-containing vesicles (PEVs) as carriers for dermal delivery of QUE. With the aim of incorporating QUE into phospholipid vesicles, commercial mixtures of phospholipids and polyethylene glycol 400 (PEG), oleic acid (OA) and their combinations were selected and used for vesicle preparation. Both terms, liposome and vesicle, can be found through the master thesis, as used in expert literature.

2 Objectives

Success of dermal application of QUE is hindered by its poor solubility in aqueous media and low skin permeability. QUE as such is inappropriate for dermal application. The aim of master thesis will be devoted to improve QUE dermal delivery, by QUE entrapment into the developed innovative vesicles. To achieve them, liposomes using different phospholipid mixtures and PEs will be designed specifically to improve QUE incorporation in liposomes and promote dermal permeability.

The aim is to prepare liposomes with various compositions and characterize them by different methods. In particular, liposome morphology in formulations will be determined by cryogenic-transmission electron microscopy and the main physico-chemical features (size, distribution and zeta potential) will be assessed by light scattering. Afterwards, drug loading efficiency will be determined by HPLC and the lipid content of the liposome dispersions will be assessed spectrophotometrically by the Stewart assay.

Once all of the data will be collected and examined, optimal formulation for *in vitro* transdermal studies will be chosen. Moreover, to check if our approach with the liposomes is successful, the penetration capability and distribution of QUE-loaded PEVs through full-thickness CD-1 mouse skin will be evaluated using Franz diffusion vertical cells.

3 Experimental work

3.1 Materials

Lipoid S 75 (S75), soybean lecithin with 70% phosphatidylcholine (and ~10% phosphatidylethanolamine, lysophosphatidylcholine 3% maximum, triglycerides 3% maximum, fatty acids 0.5% maximum, tocopherol 0.1-0.2%) and Phospholipon® 85 G (P85) soybean lecithin with minimum 85% phosphatidylcholine (and lysophosphatidylcholine 3±3%, ethanol 0.5% maximum, ethylmethylketone 500ppm maximum) were purchased from Lipoid GmbH (Ludwigshafen, Germany. Quercetin (QUE, 3,3′,4′,5,7-pentahydroxyflavone; ≥95% pure), phosphate buffer solution (PBS, pH 7.4) and polyethylene glycol 400 (PEG), oleic acid (OA), iron(III) chloride hexahydrate, ammonium thiocyanate and chloroform were purchased from Sigma-Aldrich (Milan, Italy) unless otherwise stated. All chemicals were of analytical grade. Acetonitrile, methanol, and acetic acid and water were HPLC grade and supplied by Sigma-Aldrich (Milan, Italy). CD-1 mice skin was provided by Department of Biomedical Sciences of the University of Cagliari. Twelve male mice CD1 were housed in a temperature- and humidity-controlled room with a 12-h light/dark cycle (light from 7:00 am to 7:00 pm). Animals used in this study were maintained in facilities fully accredited by the American Association for the Accreditation of Laboratory Animal Care and all experimentation was conducted in accordance with the guidelines of the Institutional Care and Use Committee of NIDA, NIH, and of the Guide for Care and Use of Laboratory Animals (National Res. Council, 1996) and the Council of the European Communities (86/ 809/EEC).

3.2 Quercetin solubility

QUE solubility was assessed by dispersing an excess amount of the drug in 5 ml of PBS or 5%, 10% v/v PEG in PBS mixtures. Dispersions were kept under constant stirring for 24 h at 25°C in a thermostated bath. After QUE excess sedimentation (18 h), the clear solutions were centrifuged for 10 minutes at 10000 rpm and the supernatant analyzed by HPLC.

3.3 Vesicle preparation and sonication

Liposomes were prepared using phospholipids S75 or P85 (180 mg/ml or 240 mg/ml) empty or loaded with QUE (10 mg/ml). With adding one of the two selected PEs (PEG or OA) or by adding both of them PEVs were obtained. PBS was used as a dispersion medium in all cases. QUE and phospholipids were weighted in a glass vial and left hydrating overnight in 3 ml of PBS (the pH adjusted to 7.4), or a mixture of PEG/PBS, OA/PBS or OA/PEG/PBS to obtain liposomes and PEVs. All vesicular dispersions were prepared and kept in the dark during the experimental time. Prior to transdermal study, PEG dispersion was prepared, dispersing 10 mg of QUE in 0.9 ml PBS and 0.1 ml PEG.

Table II lists the formulation that was prepared with PEG as a PE at different sonication conditions and number of cycles. The suspensions were sonicated (starting with 5 seconds on and 2 seconds off, 10 cycles; 13 μm of probe amplitude) with a high intensity ultrasonic disintegrator (Soniprep 150, MSE Crowley, London, UK), until yellow opalescent dispersions were obtained. Sonication continued with different number of cycles in time intervals 5 seconds on and 2 seconds off or 3 seconds on and 2 seconds off.

In this case, 0% PEG-PEVs, 5% PEG-PEVs and 10%0 PEG-PEVs containing QUE were named 1, 2, 3 respectively. First set of samples was called A (1A, 2A, 3A) the second one B (1B. 2B, 3B) and so on. Sets from A to H and set O have all the same composition and this is the formulation that was later used in *in vitro* transdermal studies. Samples with OA were named using letters I, J, K and L and samples containing OA and PEG were given letters M and N.

Table II: Liposomes with QUE and PEG as a PE. Letters A-H and O represent preparation of samples in consecutive days, n=8.

Component	**Set A – H, Set O**		
	0% PEG-PEVs (1)	**5% PEG-PEVs (2)**	**10% PEG-PEVs (3)**
S75 (mg/ml)	180	180	180
QUE (mg/ml)	10	10	10
PBS (ml)	1	0.95	0.9
PEG (ml)	-	0.05	0.1

Table III and Table IV list the formulations of prepared QUE-loaded PEVs in which OA has been used as the PE.

Table III: Liposomes with QUE and OA as the PE

Component	**Set I**				**Set J**			**Set K**			
	1	2	3	4	1	2	3	1	2	3	4
S75 (mg/ml)	180	180	-	-	180	-	-	240	240	-	-
P85 (mg/ml)	-	-	180	180	-	180	180	-	-	240	240
QUE (mg/ml)	10	10	10	10	10	10	10	10	10	10	10
OA (mg/ml)	18	36	18	36	9	9	18	12	24	12	24
PBS (ml)	1	1	1	1	1	1	1	1	1	1	1

Table IV: Liposomes with OA as the PE

Component	**Set L**						**Lipids**	
	1	2	3	4	5	6	S75	P85
S75 (mg/ml)	240	240	-	-	240	-	240	-
P85 (mg/ml)	-	-	240	240	-	240	-	240
QUE (mg/ml)	10	10	10	10	10	10	10	10
OA (mg/ml)	12	24	12	24	48	48	-	-
PBS (ml)	1	1	1	1	1	1	1	1

Furthermore, different PEs have been combined in order to obtain stable QUE-loaded vesicles. Table V presents composition of two sets of liposomes prepared with both OA and PEG as PEs.

Table V: Formulations prepared with combination of OA and PEG as PEs

Component	**Set M**		**Set N**							
	1	2	1	2	3	4	5	6	7	8
S75 (mg/ml)	240	-	240	240	-	-	240	240	-	-
P85 (mg/ml)	-	240	-	-	240	240	-	-	240	240
QUE (mg/ml)	10	10	10	10	10	10	10	10	10	10
OA (mg/ml)	12	12	12	24	12	24	12	12	12	12
PBS (ml)	0.8	0.8	0.95	0.9	0.95	0.9	0.7	0.6	0.7	0.6
PEG (ml)	0.2	0.2	0.05	0.1	0.05	0.1	0.3	0.4	0.3	0.4

Table VI: Table presenting number of sonication cycles and time intervals for all samples

	Sample	Consecutive sonication cycles						Cycles in total
Set A	1A	30 5 s on 2 s off		20	30	30 3 s on 2 s off		110
	2A	30 5 s on 2 s off		20	20	20	20 3 s on 2 s off	110
	3A	30 5 s on 2 s off		20	20	20	20 3 s on 2 s off	110
Set B	1B	90		10 5 s on 2 s off				100
	2B	90		10 5 s on 2 s off				100
	3B	90		90	90 5 s on 2 s off			270
Set C	1C	100 5 s on 2 s off						100
	2C	100 5 s on 2 s off						100
	3C	100 5 s on 2 s off						100
Set D	1D	100 5 s on 2 s off						100
	2D	100 5 s on 2 s off						100
	3D	100		100	100 5 s on 2 s off			300
Set E	1E	100 5 s on 2 s off						100
	2E	100 5 s on 2 s off						100
	3E	100		200 5 s on 2 s off				300
Set F	1F	100 5 s on 2 s off						100
	2F	100 5 s on 2 s off						100
	3F	100		100 5 s on 2 s off				200
Set G	3G	100		100	100 5 s on 2 s off		100 3 s on 2 s off	400
Set H	3H	100		100	100	100 5 s on 2 s off		400
Set O		50	10	10	10	10	10 5 s on 2 s off	100

Purification by dialysis

Non-incorporated QUE in liposome dispersions were purified by dialysis tubing (Spectra/Por® membrane: 12–14 kDa MW cut-off, 3 nm pore size; Spectrum Laboratories Inc., DG Breda, The Netherlands) against water (1000 ml) for 1 hour at room temperature**.**

Vesicles from Set O were dialyzed using the same medium that was used for their preparation, which seems more appropriate to avoid vesicle damage. Each sample (1 ml) was loaded into Spectra/Por® tubing (12–14 kDa MW cut-off; Spectrum Laboratories Inc., DG Breda, The Netherlands) and dialyzed against PBS (2 L), or PEG/PBS (5%, 10% v/v) when appropriate, which was refreshed every hour during 4 hours, at 5°C.

3.4 Vesicle characterization

Photon Correlation Spectroscopy (PCS) and Phase Analysis Light Scattering

Following dilution in a mixture of PEG and PBS (for PEG-PEVs) or in PBS (for liposomes, OA-PEVs and OA-PEG-PEVs), the average hydrodynamic diameter of the liposomes and their size distribution were determined by photon correlation spectroscopy and expressed as mean diameter (MD) and polydispersity index (PI) using a Zetasizer nano (Malvern Instrument, UK). Samples were backscattered by a helium-neon laser (633nm) at an angle of 173° and a constant temperature of 25°C. The PI represents a measure of the width of the size distribution. The lower is the PI the smaller the size distribution. Increased PI may be a result of clusters or non-entrapped QUE. Optimum PI should be below 0.1 and it indicates a homogenous and monodisperse population. However, PI less than 0.3 are generally considered acceptable. Surface charge was measured using the Zetasizer nano by means of the M3-PALS (Mixed Mode Measurement - Phase Analysis Light Scattering) technique, which measures the particle electrophoretic mobility in a thermostated cell. All experiments were performed in triplicate and results are presented as mean ± S.D.

Cryogenic-Transmission Electron Microscopy (Cryo-TEM)

Vesicle formation and morphology were checked by cryogenic transmission electron microscopy (cryo-TEM). For the analysis, a thin aqueous film was formed by placing 5 µl of the vesicular dispersion on a glow-discharged holey carbon grid, and then blotting the grid against filter paper. The resulting thin sample film spanning the grid holes were vitrified by plunging the grid (kept at 100% humidity and room temperature) into ethane, maintained at its melting point with liquid nitrogen, using a Vitrobot (FEI Company, Eindhoven, The Netherlands). The vitreous film was transferred to a Tecnai F20 TEM (FEI Company, Eindhoven, The Netherlands) using a Gatan cryo-transfer (Gatan, Pleasanton, CA), and the sample was observed in a low-dose mode. Images were acquired at 200 kV at a temperature of –170/–175 °C, using low-dose imaging conditions not exceeding 20 e^{-} /$Å^2$, with a 4096 × 4096 pixel CCD Eagle camera (FEI Company, Eindhoven, The Netherlands).

HPLC for determining of QUE loading efficiency

Liposomes samples after dialysis were dissolved in methanol in ratio 1:100 and injected into the HPLC system and analyzed. QUE content was quantified by reversed-phase high performance liquid chromatography (HPLC) at 255 and 367 nm using the chromatograph Alliance 2690 (Waters, Milan, Italy), equipped with a photodiode array detector and a computer integrating apparatus (Empower 3). The column was a SunFire C18 (3.5µm, 4.6 x 150 mm, Waters, Italy). The mobile phase was a mixture of acetonitrile, water and acetic acid (94.8:5:0.2, v/v), delivered at a flow rate of 1.0 ml/min and a run time 10 min.

Entrapment efficiency (EE %, *Equation 1*) represents the amount of drug actually entrapped into the liposomes after dialysis and it is expressed as a percentage of the amount of QUE initially used. EE % was using the following formula:

$$EE\ (\%) = \frac{Determined\ amount\ of\ QUE\ in\ liposomes}{Theoretical\ amount\ of\ QUE\ in\ liposomes} \times 100 \qquad \textit{(Equation 1)}$$

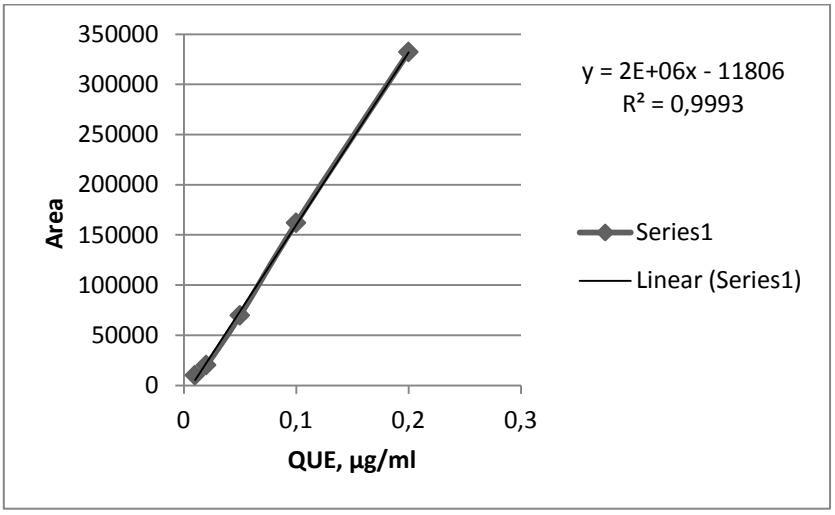

Figure 5: Calibration graph for quantitative determination of QUE

Stewart Assay (Colorimetric Determination of Phospholipids in dispersion with Ammonium Ferrothiocyanate)

The lipid content of the dispersions was determined by a method based on the formation of the complex between ammonium ferrothiocyanate and phospholipids. The method allows measurements of phospholipids in the range 0.01 – 0.10 mg/ml. A standard solution of ammonium ferrothiocyanate was prepared by dissolving 2.70 g ferric chloride hexahydrate and 3.04 g ammonium thiocyanate in distilled water and making up to 100 ml. An aliquot of liposomes and PEVs suspensions was added to a biphasic mixture of aqueous ammonium ferrothiocyanate solution and chloroform. The concentration of S75 was obtained by measuring absorbance at 485 nm into the organic chloroform layer using UV/VIS Spectrometer, Perkin Elmer, Italy. The standard curve was used to determine phospholipid content of each aliquot (Figure 6). The aggregation efficiency (AE%) represented the effective amount of aggregated phospholipids expressed as the percentage of the amount initially used.

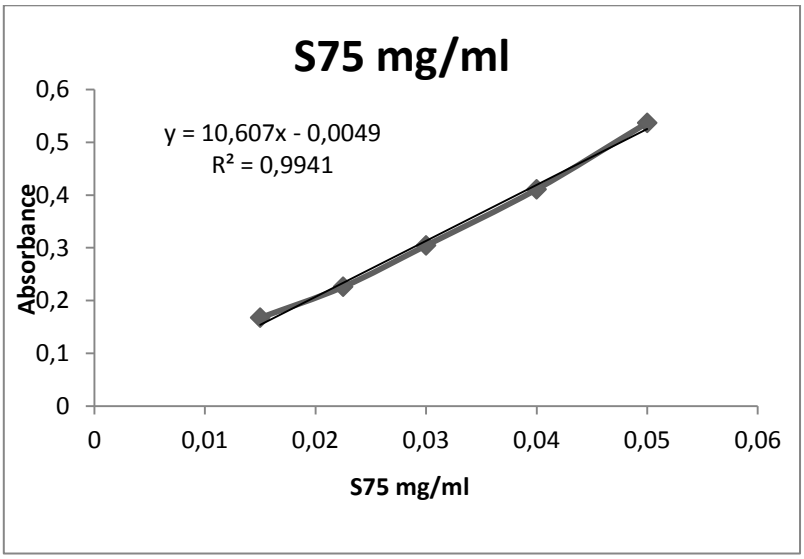

Figure 6: Calibration graph for calorimetric determination of phospholipids in dispersion

3.5 *In vitro* skin permeation studies

Experiments were performed non-occlusively by Franz diffusion vertical cells (Colaver, Vimodrone, Milan, Italy) with an effective diffusion area of 0.785 cm^2, using twenty days

old CD-1 mice's skin. The skin, previously stored at -80 °C, was pre-equilibrated in saline at 25 °C, 16 hours before the experiments. Skin specimens (n=4 per formulation) were sandwiched securely between donor and receptor compartments of the Franz cell, with the stratum corneum side facing the donor compartment. The acceptor compartment was filled with 5.5 ml of saline, which was continuously stirred with a small magnetic bar and thermostated at 37± 1 °C throughout the experiments to reach the physiological skin temperature (*i.e*. 32 ± 1 °C).

Twenty microliters of the tested vesicle suspensions was placed onto each skin surface. The samples from receptor medium were withdrawn after the first and the second hour and then every two hours up to eight hours after the beginning of the experiment. Every time, the withdrawn receiving solution was replaced with an equivalent volume of fresh saline. Last withdrawal was done twenty-four hours after the beginning of the experiments. Withdrawn receiving solutions were analyzed by HPLC for drug content.

After 24h, the skin surface of specimens was dried with paper and on air. The stratum corneum was removed by stripping with adhesive tape. Each piece of the adhesive tape (Tesa® film, Beiersdorf, Germany) was firmly pressed on the skin surface and rapidly pulled off with the fluent stroke. Nine stripping procedures were performed consecutively. Epidermis was separated from dermis with a surgical scalpel. Stratum corneum tape strips, epidermis and dermis were cut and placed in distinct flasks. 3 ml of methanol were added to stratum corneum and 2 ml of methanol were added to epidermis and dermis each. Samples were sonicated with Soniprep 150 ultrasonic disintegrator (MSE, Crowley, UK) 2 cycles (60 seconds on, 20 seconds off) to extract the drug and then the mixtures were filtered and each solution assayed for drug content by HPLC.

Statistical analysis of data

Data analysis was carried out with the software package R, version 2.10.1. Results are expressed as the mean ± standard deviation (SD) of X replicates coming from different preparation batches. Multiple comparisons of means (Turkey test) were used to substantiate statistical differences between groups, while Student's t-test was applied for comparison between two samples. Significance was tested at the 0.05 level probability (p).

4 Results and Discussion

In the present work, as to provide suitable carrier system for dermal application of QUE, innovative liposomes were studied. We have prepared and tested liposomes with combining QUE, PEG, OA and soybean phospholipids containing 70% (Lipoid S 75) or 85% phosphatidylcholine (Phospholipon® 85) using sonication method. The vesicle lipid composition and structure and their influence on their performances was evaluated.

4.1 QUE solubility

It is known that the water solubility of QUE is extremely low (less than 10 μg/ml) despite the fact that possesses 5 hydroxyl (-OH) functional groups, which offer possibilities for formation of bonds with polar character such as dipole-dipole interactions and hydrogen bonds. Considering this, QUE should be well soluble in polar, particularly in protic, solvents like water, methanol, ethanol. Moreover, also carbonyl and pyran oxygen may contribute to interactions. Another relevant fact that affects QUE susceptibility is the molecule's flexibility. We can see from the Figure 7 that major part of QUE molecule is planar and maximum rotation will occur at the single bond that connects the B ring to the C ring. Additionally, pyran oxygen is obscured with the hydrophobic part of the molecule. However, different values can be found in literature for water solubility of QUE. While Li et al report the value of 7.7 μg/ml (24) for solubility of QUE in water, Cadena et al also investigated drug's solubility and obtained much lower value of 0.3 μg/ml (41).

PBS was used as a dispersion medium throughout our experiments, since it has been shown that QUE solubility in PBS is greater than in water. Estimated negative logarithms of QUE dissociation constants are pKa1 = 7.17, pKa2 = 8.26, pKa3 = 10.13, pKa4 = 12.30, pKa5 = 13.11 (42). At pH 7.4 in PBS, slight ionization of QUE occurs and therefore the increase in solubility. pH-dependent solubility can be expected since the QUE molecule can ionize phenolic hydroxyl groups. QUE behaves as a weak acid. When pH is lower, phenolic hydroxyl groups are not ionized, because the free H^+ ion tends to keep them in their non-ionic state. As pH increases, concentration of H^+ ion decreases and the QUE molecule is being ionized. This heads to an increase in its solubility (41). Solvent accessible surface is presented in Figure 8.

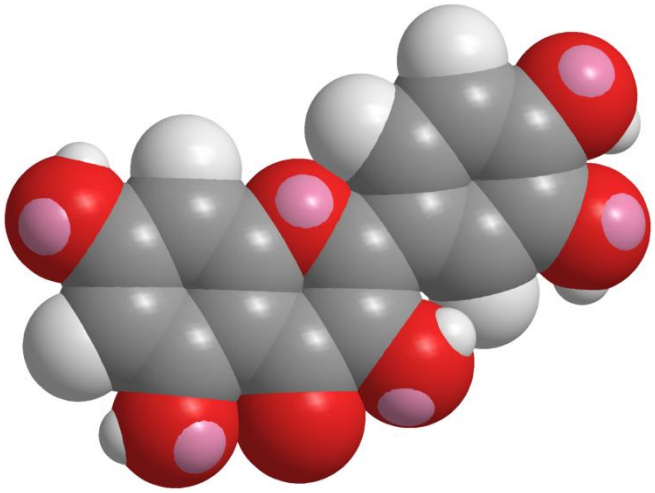

Figure 7: Space-filling model of QUE

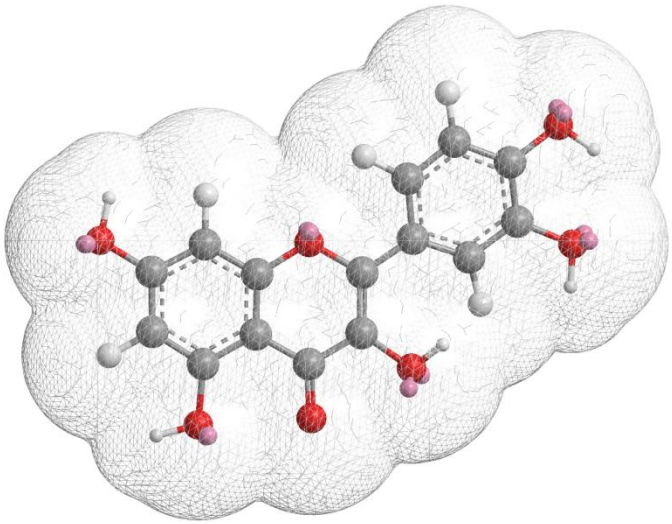

Figure 8: QUE solvent accessible surface

In the present study, experimental results for QUE solubility in PBS and in PEG-PBS solution (5% and 10%) showed increase in solubility as a function of PEG. The presence of PEG increased drug solubility by 3.5- and 5.1-fold with 5% and 10% PEG, respectively, which can be seen in Table VII. Compared to Cadena et al, our result for QUE solubility in PBS is 4.2-fold greater. PEG is highly hydrophilic substance, its partition coefficient between hexane and water is 0.000015, and it is able to form favourable interactions, especially if the –OH groups are deprotonated.

Table VII: QUE solubility in PBS or PEG/PBS mixtures (5 and 10% v/v). Values are the means ± standard deviation (n=3)

Medium	**Quercetin (µg/ml)**
PBS	9.3 ± 0.11
5% PEG in PBS	32.7 ± 5.37
10% PEG in PBS	47.5 ± 5.20

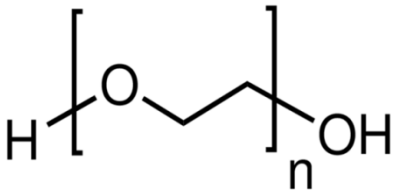

Figure 9: Polyethylene glycol chemical structure

4.2 Effect of sonication on vesicle size

In an attempt to improve dermal delivery of QUE, sonicated vesicular formulations, containing PEG, OA or both of them, have been prepared.

Sonication of samples from set "A" started with 30 cycles at 5 s on 2 s off. After the analysis of results, sonication continued for four times with 20 cycles for samples 2A and 3A, until completing 110 cycles in total. In addition to initial 30 cycles, 20 cycles were given to sample 1A and after that another two times of 30 cycles (3 s on 2 s off) were applied until completing 110 cycles. Vesicle size, PI and ZP were characterized using Zetasizer nano. Sonication steps for all samples are summarized in Table VI.

Table VIII presents the data obtained with first set of formulations after characterizing the size. Results of the preliminary study of formulations of QUE-loaded vesicles showed that in general the higher the number of sonication cycles the smaller the vesicles.

However, in the case of liposomes, the smallest vesicles were obtained with 30 cycles. Afterward, the vesicle size increased. When the PEG-PEVs were tested, the main results using 10% PEG was that vesicle size was very large even after 110 cycles of sonication

that were able to reduce vesicle size to only more than 1 μm (Figure 10). On the contrary, 5% PEG-PEVs showed a smaller size. Moreover, all these systems showed high polydispersity index, which represent wide size distribution of vesicles.

Table VIII: Mean diameter (MD) and polydispersity index (PI) of set A of QUE-loaded PEG-PEVs

	Sample 1A, 0% PEG-PEVs		**Sample 2A, 5% PEG-PEVs**		**Sample 3A, 10% PEG-PEVs**	
Cycles	MD (nm)	PI	MD (nm)	PI	MD (nm)	PI
30	163 ± 7	0.51	361 ± 28	0.85	2821 ± 204	0.55
50	273 ± 66	0.42	283 ± 23	0.74	2585 ± 17	0.98
70	-	-	402 ± 82	0.72	2588 ± 403	0.74
80	242 ± 32	0.64	-	-	-	-
90	-	-	303 ± 38	0.65	1505 ± 294	0.86
110	264 ± 32	0.37	325 ± 55	0.64	1341 ± 256	0.96

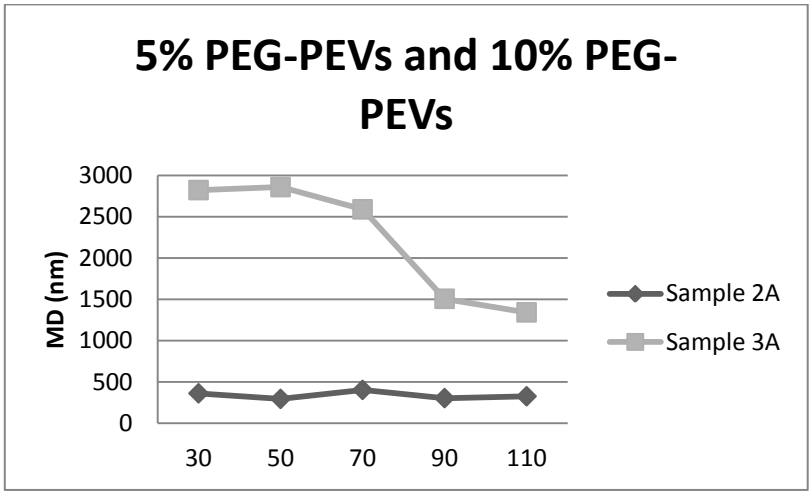

Figure 10: Linear chart representing 5% PEG-PEVs' and 10% PEG-PEVs' MDs and corresponding sonication cycles

Continuing preparing samples and determining mean diameter and polydispersity index, we obtained results of sets B-F, which are presented in tables IX – XIV.

Table IX: Characteristics of second set of QUE-loaded PEVs: mean diameter (MD) and polydispersity index (PI)

Cycles	**Sample 1B, 0% PEG-PEVs**		**Sample 2B, 5% PEG-PEVs**		**Sample 3B, 10% PEG-PEVs**	
	MD (nm)	PI	MD (nm)	PI	MD (nm)	PI
90	119 ± 5	0.45	169 ± 10	0.57	934 ± 185	1.00
100	123 ± 8	0.40	170 ± 6	0.66	-	-
180	-	-	-	-	412 ± 72	0.97
270	-	-	-	-	529 ± 82	1.00

Table X: Characteristics of third set of QUE-loaded PEVs: mean diameter (MD) and polydispersity index (PI)

Cycles	**Sample 1C, 0% PEG-PEVs**		**Sample 2C, 5% PEG-PEVs**		**Sample 3C, 10% PEG-PEVs**	
	MD (nm)	PI	MD (nm)	PI	MD (nm)	PI
100	126 ± 7	0.40	136 ± 5	0.42	297 ± 14	0.83

Table XI: Characteristics of fourth set of QUE-loaded PEVs: mean diameter (MD) and polydispersity index (PI) and zeta potential (ZP)

Cycles	**Sample 1D, 0% PEG-PEVs**			**Sample 2D, 5% PEG-PEVs**			**Sample 3D, 10% PEG-PEVs**		
	MD (nm)	PI	ZP (mV)	MD (nm)	PI	ZP (mV)	MD (nm)	PI	ZP (mV)
100	122 ± 6	0.42	- 8 ± 0.3	161 ± 10	0.44	- 5 ± 0.3	642 ± 237	0.95	-
200	-	-	-	-	-	-	424 ± 23	0.85	-
300	-	-	-	-	-	-	355 ± 56	0.84	- 3 ± 0.2

Table XII: Characteristics of fifth set of QUE-loaded PEVs: mean diameter (MD) and polydispersity index (PI) and zeta potential (ZP)

Cycles	**Sample 1E, 0% PEG-PEVs**			**Sample 2E, 5% PEG-PEVs**			**Sample 3E, 10% PEG-PEVs**		
	MD (nm)	PI	ZP (mV)	MD (nm)	PI	ZP (mV)	MD (nm)	PI	ZP (mV)
100	140 ± 15	0.48	- 5 ± 1.1	156 ± 20	0.46	- 4 ± 0.5	766 ± 89	1.00	-
300	-	-	-	-	-	-	506 ± 120	0.89	- 4 ± 0.1

Table XIII: Characteristics of QUE-loaded PEVs that were used in (trans)dermal studies: mean diameter (MD), polydispersity index (PI) and zeta potential (ZP)

Cycles	**Sample 1F, 0% PEG-PEVs**			**Sample 2F, 5% PEG-PEVs**		
	MD (nm)	PI	ZP (mV)	MD (nm)	PI	ZP (mV)
100	128 ± 13	0.43	-8 ± 0.4	328 ± 31	0.94	- 6 ± 0.3

Table XIV: Characteristics of 3G and 3H, 10% PEG-PEVs: mean diameter (MD), polydispersity index (PI) and zeta potential (ZP)

Cycles	**Sample 3G, 10% PEG-PEVs**		**Sample 3H, 10% PEG-PEVs**		
	MD (nm)	PI	MD (nm)	PI	ZP (mV)
100	1026 ± 205	1.0	797 ± 124	0.95	-
200	1169 ± 186	0.98	708 ± 38	0.70	-
300	704 ± 159	0.94	474 ± 44	0.60	-
400	680 ± 85	0.84	315 ± 53	0.74	- 6 ± 0.4

Sample 3G presented too high MD and also PI, which did not achieve suitable values after sonicating sample four times for 100 cycles. Sample 3H, 10% PEG-PEVs that were used in transdermal studies, showed high vesicle size after first 100 cycles. We have continued adding 100 cycles for another three times and we obtained vesicles with size of

approximately 300 nm, what can be seen in Table XIV and Figure 11. We also managed to lower PI, which was, however, still much too high after 400 cycles.

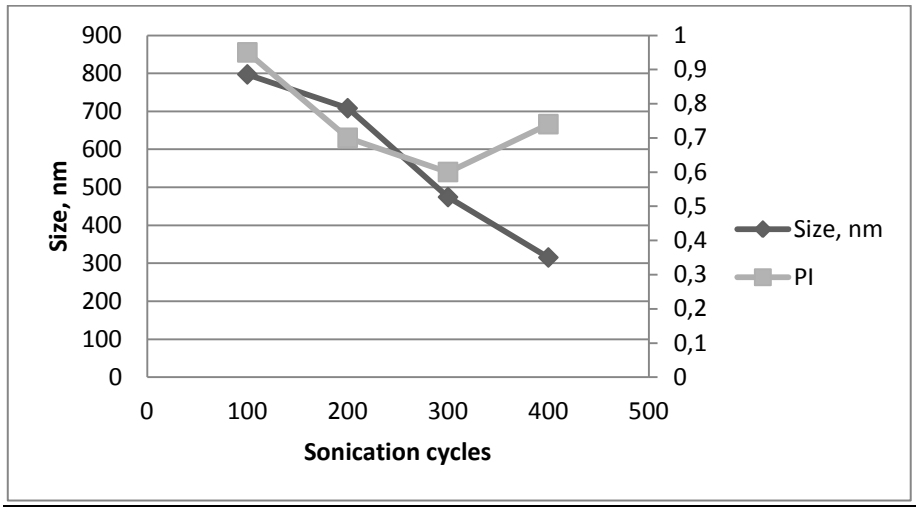

Figure 11: Linear chart representing mean diameter and polydispersity index of 10% PEG-PEVs' used in *in vitro* studies and corresponding sonication cycles (sample 3H)

In order to find another suitable formulation to perform *in vitro* studies with, oleic acid (OA) was used as a penetration enhancer in samples I, J, K and L. All the formulations were first sonicated 20 cycles 5 seconds on and 2 seconds off and after this, another 20 cycles of 3 s on 2 s off were added. Also all of the following cycles were of 3s on 2 s off. When observing samples it was evident that both formulations prepared with 36 mg/ml of OA (20%) were unable to form liposomes. Both of them formed gel and in sample I2 some PBS was left free. Sample I3, which was the only one within the small size (193 nm after 40 cycles), but one day after the phase separation was observed.

Research continued preparing and investigating samples containing 5% and 10% of OA.

Table XV: Characteristics of prepared formulations with S75 and P85 and OA as PE

Cycles	**Sample J1**		**Sample J2**		**Sample J3**	
	MD (nm)	PI	MD (nm)	PI	MD (nm)	PI
20	197 ± 12	0.46	176 ± 15	0.44	201 ± 2	0.48
40	155 ± 7	0.46	159 ± 4	0.52	209 ± 58	0.49
60	171 ± 14	0.49	196 ± 16	0.57	190 ± 23	0.43
ZP (mV)	- 19 ± 1.1		- 18 ± 0.2		- 22 ± 0.5	

It can be seen from Table XV that formulations from set J, prepared with 9 mg/ml (5%) of OA, presented smaller MD compared to those prepared with 18 mg/ml (10%) of OA. However, PI was in all cases around 0.5 which is considered too high and in general three peaks were observed in each formulation. ZP values were all negative and around -20mV, but observations made five days after preparing liposomes showed that all of them were unstable.

In all of the following sets increased quantity of phospholipids was used (240 mg/ml instead of 180mg/ml like in previous samples).

Table XVI: Characteristics of prepared formulations with 240 mg S 75 or P 85 and OA as PE

Cycles	**Sample K1**		**Sample K2**		**Sample K3**		**Sample K4**	
	MD (nm)	PI	MD (nm)	PI.	MD (nm)	PI	MD (nm)	PI
20	132 ± 2	0.30	148 ± 1	0.24	167± 24	0.42	160 ±4	0.38
40	-	-	-	-	133 ± 8	0.41	154 ± 3	0.32
60	-	-	-	-	124 ± 8	0.40	159 ± 5	0.37

Values acquired by set K samples characterization were promising. They are summarized in Table XVI and we can see that OA-PEVs were never greater than 170 nm in mean diameter and PI was from 0.24 to 0.42. After Set K results were obtained, we decided to re-prepare the formulations.

Samples from L1 to L4, consisting of 240 mg/ml of S75 or P85 and OA (5% or 10%), have the same compositions as samples K1-K4 and their characteristics are listed in Table XVII. Two times 10 cycles of 5 s on, 2 s off have been given to formulations at first. Next 20 cycles were 3 s on 2 s off. Sample L2 resulted too dense to measure MD and PI, sample L5 became dense like gel and sample L6 remained fixed on vial walls.

Few days after obtaining measurements visual observations were carried out. Nevertheless suitable size and almost suitable PI, samples K1 and K3 have separated totally and in K2 a lot of QUE have been visible free, also on vial bottom. Separation of phases occurred in all of the set L samples that seemed promising after sonication, and the same happened to lipids formulations.

Table XVII: Characteristics of set L

Cycles	**Sample L1**		**Sample L2**		**Sample L3**		**Sample L4**	
	MD (nm)	PI	MD (nm)	PI	MD (nm)	PI	MD (nm)	PI
20	165 ± 7	0.32	*To dense to measure*		146 ± 1	0.40	159 ±3	0.30
40	143 ± 6	0.33	-	-	145 ± 4	0.49	163 ± 2	0.40

Table XVIII: Characteristics of lipids

Cycles	**Sample LIPIDS S 75**			**Sample LIPIDS P 85**		
	MD (nm)	PI	ZP (mV)	MD (nm)	PI	ZP (mV)
20	130 ± 11	0.40	- 10 ± 0.2	1441 ± 4	0.46	- 12 ± 0.5

Formulations from set M were prepared by using combination of both OA and PEG (1:4). After 10 and another 20 cycles 5 s on 2 s off have been given to samples, they solidified and no size data could be obtained.

Also samples in set N are containing both OA and PEG (1:1, 1:6, 1:8) and their characteristics are presented in Table XIX. Size, PI and ZP could not have been obtained for samples N5-8, (OA:PEG 1:6, 1:8) since they solidified during preparation.

Table XIX: MD, PI and ZP of set N

Cycles	**Sample N1**			**Sample N3**		
	MD (nm)	PI	ZP (mV)	MD (nm)	PI	ZP (mV)
20	214 ± 2	0.35	- 17 ± 0.6	214 ± 3	0.38	- 13 ± 0.6
50	208 ± 1	0.38	- 14 ± 0.9	200 ± 20	0.35	- 12 ± 0.3
Cycles	**Sample N2**			**Sample N4**		
	MD (nm)	PI	ZP (mV)	MD (nm)	PI	ZP (mV)
30	359 ± 6	0.75	- 11 ± 1.3	741 ± 9	0.73	- 8 ± 0.08

When revising characterization data of samples containing OA and both OA and PEG as PE, it was obvious that no sample suitable for *in vitro* transdermal experiments was

obtained. Formulations prepared with 180 mg/ml of phospholipids and 10% or 20% OA were not able to form liposomes. Yet, improvements were achieved in formulations with 240 mg/ml of phospholipid where majority of samples did show suitable size and PI, but lacked appropriate stability. It is well known that a highly negative or positive surface charge (± 30 mV) is indicative of high particle stability against aggregation and fusion. However, in this case, all formulations showed a lower ZP value, including the formulations containing OA, which was used to improve stabilization. In this last case, although the more negative ZP, the quick deposition could be due to negative interactions between the OA and the drug.

Samples that proceeded to *in vitro* transdermal study were prepared with 180 mg/ml of S75 containing 10 mg/ml of QUE and 0% (sample 1F), 5% (sample 2F) or 10% (sample 3H) of PEG. However, not all of the samples demonstrated desired characteristics. Both 5% PEG-PEVs and 10% PEG-PEVs were much too polydisperse (PI 0.97 and 0.74, respectively). Nevertheless, samples were used in transdermal study, because all of the different samples had to be tested *in vitro,* even if its characterization data were not good.

4.3 Effect of dialysis on vesicle size trend

The results have shown that the size of post-dialysed vesicles with QUE decreased, as is presented in Table XX, except in case of 10% PEG-PEVs. They presented less negative ZP values compared to liposomes and 5% PEG-PEVs. As regards stability behavior of a colloid, ZP values from 0 ± 5 mV normally lead to rapid coagulation and flocculation. Neutralizing the electric charge of the dispersed phase particles lead to aggregation. This happened in case of 10% PEG-PEVs, where we can observe increase in MD for more than 500 nm.

Table XX: Characteristics of QUE-loaded PEVs before and after the dialysis: mean diameter (MD) and polydispersity index (PI) and zeta potential (ZP)

Sample		Mean diameter (nm)	PI	ZP (mV)
Liposomes (1F)	Pre-dialysis	128 ± 13	0.43	-8 ± 0.4
	Post- dialysis	124 ± 3	0.46	-7 ± 0.2
5% PEG-PEVs (2F)	Pre-dialysis	328 ± 31	0.94	- 6 ± 0.3
	Post- dialysis	170 ± 10	0.52	- 5 ± 1
10% PEG-PEVs (3F)	Pre-dialysis	319 ± 34	0.86	- 4 ± 0.2
	Post- dialysis	840 ± 116	0.97	- 4 ± 0.2

4.4 Characteristics of the vesicles with PE

Dynamic Laser Light Scattering results, summarized in Table XXI show an increase (P<0.05) in the mean diameter of the prepared vesicles, as a function of the presence of loaded QUE and PEG (the higher its concentration, the larger the vesicles).

Table XXI: Characteristics of empty and QUE-loaded liposomes and PEVs with PEG (Set O): mean diameter (MD), polydispersity index (PI), zeta potential (ZP), entrapment efficiency (EE%) and aggregation efficiency (AE%). Values are the means ± standard deviation. *MD, PI and ZP values of Set O, EE% and AE% of Sets D, E, F

Sample		MD (nm)	PI	ZP (mV)	EE%	AE%
Liposomes	empty	96 ± 2.4	0.22	-9 ± 0.5		
	QUE	116 ± 5.3	0.35	-9 ± 0.4	52 ± 4.4	74 ± 4.6
5%PEG-PEVs	empty	117 ± 5.7	0.23	-10 ± 0.8		
	QUE	152 ± 2.4	0.34	-10 ± 0.8	75 ± 3.0	71 ± 2.7
10%PEG-PEVs	empty	136 ± 2.6	0.23	-9 ± 0.8		
	QUE	148 ± 3.5	0.31	-10 ± 0.7	60 ± 0.8	73 ± 6.3

QUE-loaded vesicles have had always bigger mean diameters compared to empty vesicles. Nevertheless, the vesicles were small in size, between 100 and 150 nm, with acceptable and repeatable homogeneity (PI ≤0.35), and zeta potential values slightly negative (-10 mV), due to the low charge carried by Lipoid S75. The presence of PEG increased drug entrapment efficiency of vesicles, which was especially true in the case of 5% PEG-PEVs (75% *vs* 52% for control liposomes). Aggregation efficiency data obtained from Stewart assay showed that about 70% of phospholipids were aggregated to form vesicles.

Dynamic Laser Light Scattering results, presented in Table XXII, show an increase in the mean diameter of the prepared liposomes and OA-containing vesicles as a function of OA and the presence of P85. Mean diameters were small, from 130 nm to 159 nm and MD of liposomes and PEVs prepared with P85 is always greater compared to S75. PI of samples prepared with S75 (ranging from 0.24 to 0.40) was always lower compared to formulations with P85 (from 0.39 to 0.49) and showed a decrease as a function of OA. Surface charge presented by ZP values was slightly negative (around -11 mV) in control liposomes containing S75 and P85 as well.

Table XXII: Characteristics of S75 and P85 QUE-loaded liposomes and PEVs with OA: mean diameter (MD), polydispersity index (PI), zeta potential (ZP). Values are the means ± standard deviation (n = 3).

Sample		**MD (nm)**	**PI**	**ZP (mV)**
Liposomes	**S75 (Lipids S75)**	130 ± 11	0.40	- 10 ± 0.2
	P85 (Lipids P85)	144 ± 4	0.46	- 12 ± 0.5
5%OA-PEVs	**S75 (L1)**	143 ± 6	0.33	/
	P85 (L3)	145 ± 4	0.49	/
10%OA-PEVs	**S75 (K2)**	148 ± 1	0.24	/
	P85 (K4)	159 ± 5	0.37	/

Liposomes used for *in vitro* transdermal studies were selected based on the results of the physico-chemical characterization of the prepared dispersions that included the evaluation of vesicle stability, MD and size distribution of the vesicles, ZP, and the results of the entrapment efficiency as well as final lipid content of the carriers. Formulations that

contain OA as PE and as well formulations containing both OA and PEG as PEs did not proceed to *in vitro* studies, because none of them presented required stability.

4.4.1 Effect of PEG and OA on vesicle size

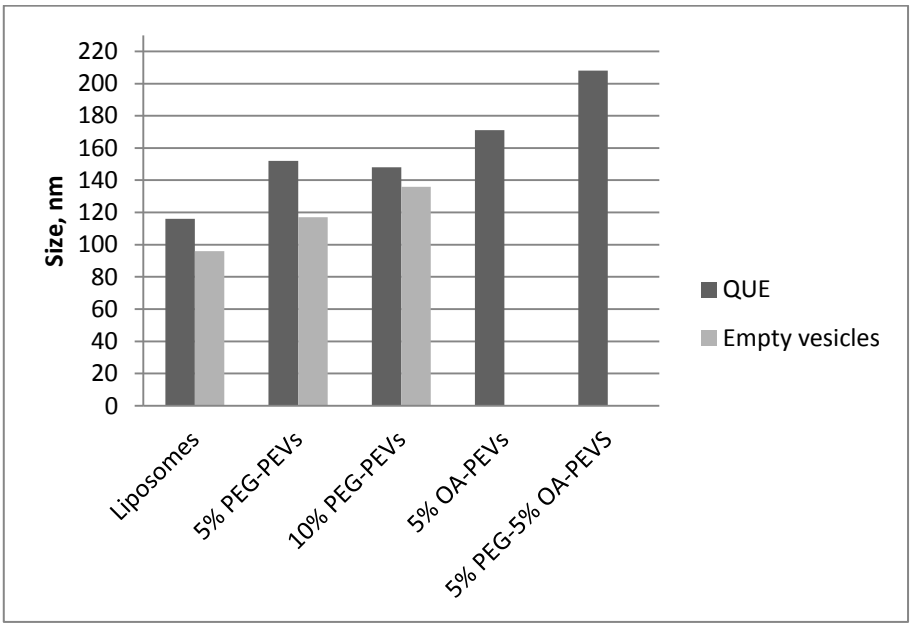

Figure 12: Effect of PEG or OA used in preparation of empty and QUE-loaded vesicles on vesicle size (Liposomes having the composition of sets A-F (being sample 1O), 5% PEG-PEVS having the composition of 2A-F (sample 2O), 10% PEG-PEVs having the composition of sets 3A-H (sample 3O), 5% OA-PEVs being sample J1 5% PEG-5% OA-PEVS being sample N1)

Results presented in Figure 12 show an increase ($P<0.05$) in average diameter of the prepared vesicles as a function of the presence of loaded QUE and addition of the PE. Increase in MD was more evident when PEs were simultaneously used in 5% PEG-5% OA-PEVs. From the Figure 12 we can see that there is not much difference in vesicle size when comparing 5% PEG-PEVs and 10% PEG-PEVs. However, there is a slight increase in size in vesicles containing OA, for approximately 20 nm according to 5% PEG-PEVs and 10% PEG-PEVs. Sample J1 contains 5% OA with 180 mg/ml S75. Sample N1 contains 5% of OA and 5% of PEG, combined with S75 and show increase in size compared to all of the other samples.

4.4.2 Effect of PE on surface charge (ZP)

Samples presented in Figure 13, where negative surface charge values are presented, have been all prepared with S75, which carries a low charge. We can see that ZP of liposomes and PEG-PEVs are similar, while there is an increase in surface charge of OA-PEVs. The most negative surface charge was found in sample J1 which was prepared with 5% OA. Irrespective of more negative surface charge, the sample did not show desired stability.

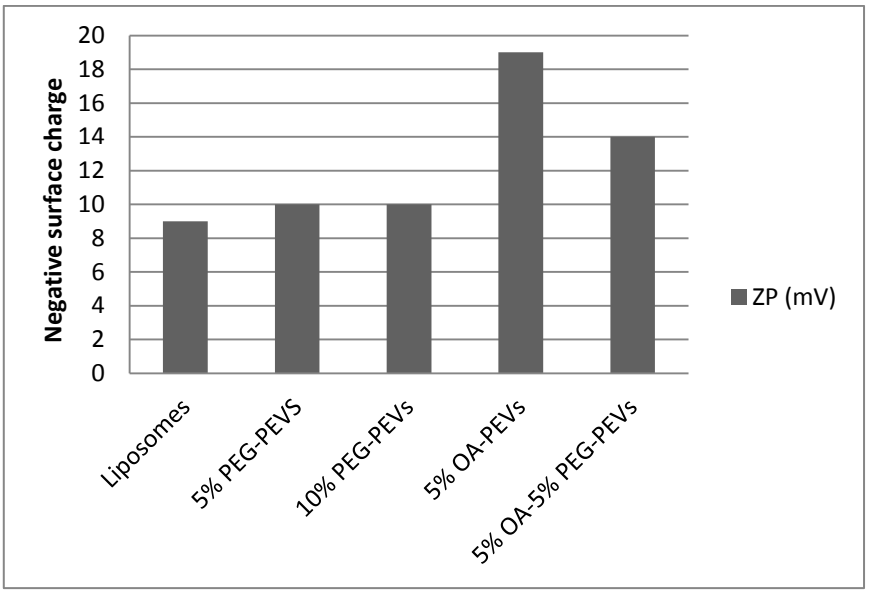

Figure 13: Effect of PEG and OA on surface charge of PEVs compared to liposomes

4.4.3 Effect of vesicle composition on entrapment efficiencies of QUE

The presence of PEG increased the entrapment efficiency of QUE in vesicles. The experiments regarding QUE solubility showed that this physical property of the drug greatly increased in the dispersion media used in the vesicle preparation. This and the solubilising power of the vesicles are responsible for the high entrapment efficiencies found during this research, ranging between 52% for control liposomes and 75% for 5% PEG-PEVs (Figure 14). Moreover, after the dialysis procedure no drug crystals were shown by the cryo-TEM images thus demonstrating the actual entrapment of QUE in the studied vesicles.

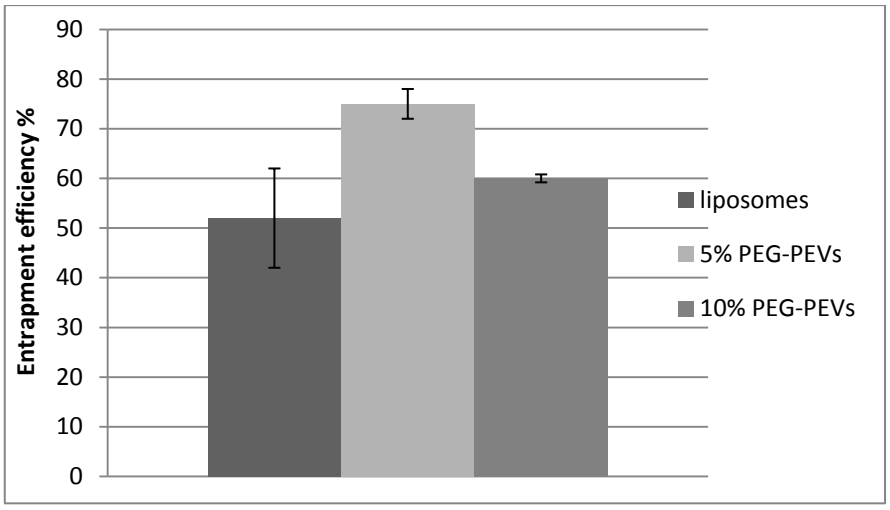

Figure 14: Entrapment efficiency of quercetin in liposomes and PEVs

4.5 Morphology of vesicles

Cryo-TEM observation was used for investigation of size, shape and lamellarity of sonicated 5% PEG-PEVs and 10% PEG-PEVs. Owing to the relatively high contrast of the phospholipid bilayer, liposomes appear as typical ring-shaped structures in cryo-TEM images. Analysis confirmed the formations of small and fairly spherical vesicles with different lamellarity directly proportional to PEG content. Greater lamellarity is observed in 10% PEG-PEVs sample than in 5% PEG-PEVs. There was no evidence of free QUE crystals. Figure 15 illustrate a heterogeneous population of concentric small and large unilamellar, oligolamellar and multilamellar structures of approximately 150-200 nm in diameter. This value is consistent with those determined by size measurements.

Some invaginated vesicles are present, which are probably due to the occurrence of ionic gradients during sample processing. Liposome shape may be influenced by the rigidity of the lipid bilayer and consequently vesicle deformation and invaginations can occur when the lipid bilayer is extremely flexible.

a)

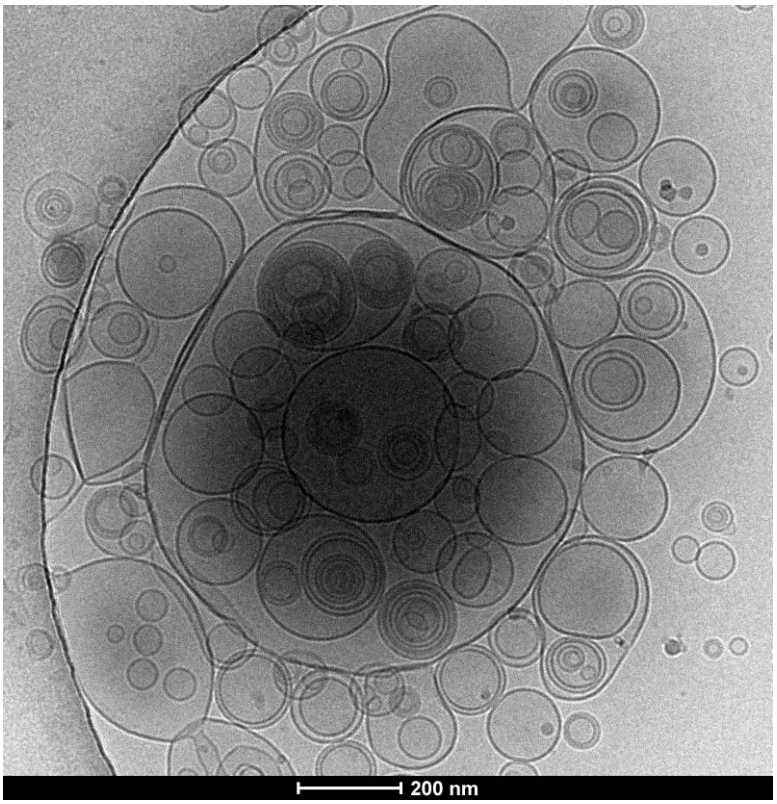

b)

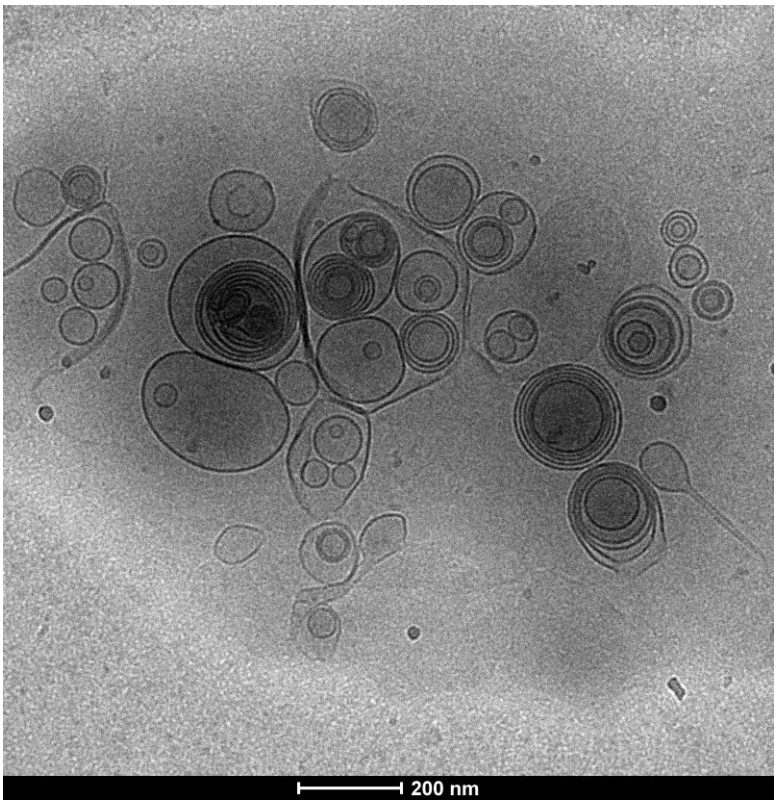

Figure 15: Cryo-TEM micrograph of sonicated 5% PEG-PEVs, sample 2D (a) and 10% PEG-PEVs (b)

4.6 *In vitro* transdermal penetration of QUE

In order to evaluate the influence of composition, structure and surface charge of the studied liposomes on the QUE penetration into and diffusion through the skin, we carried out *in vitro* studies using mouse skin and vertical Franz diffusion cells. The amount of QUE accumulated into stratum corneum (SC), epidermis, and dermis is expressed as the percentage of the drug applied onto the skin.

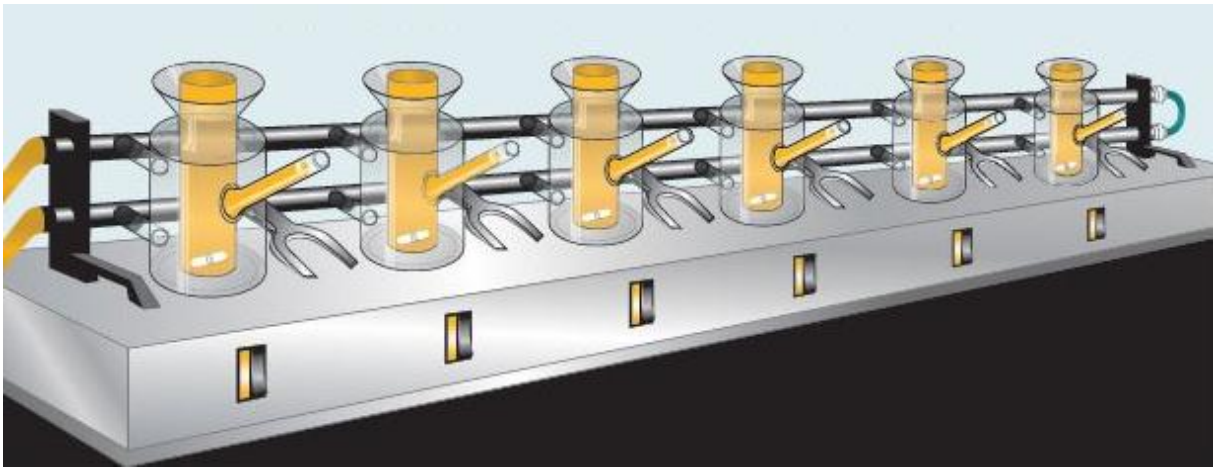

Figure 16: Multi-station Franz diffusion cell system (75)

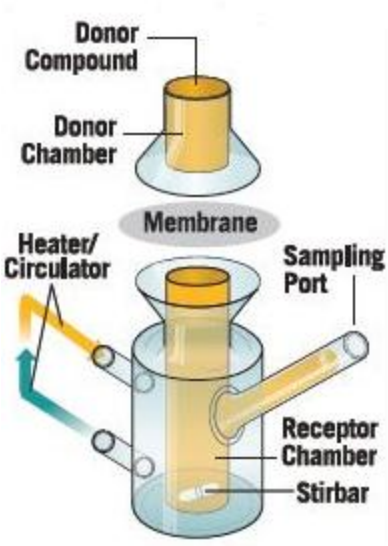

Figure 17: Franz diffusion vertical cell (75)

From the Figure 18 is seen that percentage of accumulated QUE in skin layers is very low (less than 1% in total with all of the samples). The highest accumulation of quercetin was reached in the stratum corneum (SC), with a minimum value (≈ 0.22%) for 5% PEG-PEVs and PEG dispersion and a maximum value (≈ 0.28%) for 10% PEG-PEVs. No statistically significant enhancement of accumulation was demonstrated among the control liposomes, PEG-PEVs and PEG dispersion after the *in vitro* transdermal study ($p>0.05$) except for 5% PEG-PEVs that showed the lowest accumulation values in comparison with the other formulations. Moreover, the total mean amount of QUE deposited into the skin was always higher in the SC than in epidermis and dermis. Nevertheless, no statistical differences could be found in the amount of the drug accumulated in the different skin strata ($p>0.05$) except in the case of liposomes, 5% and 10% PEG-PEVs that showed QUE accumulation in the dermis statistically lower than in SC and epidermis. On the contrary, PEG dispersion led to a deposition in dermis similar to that in the epidermis and is not statistically significant ($p>0.05$) also in comparison with SC.

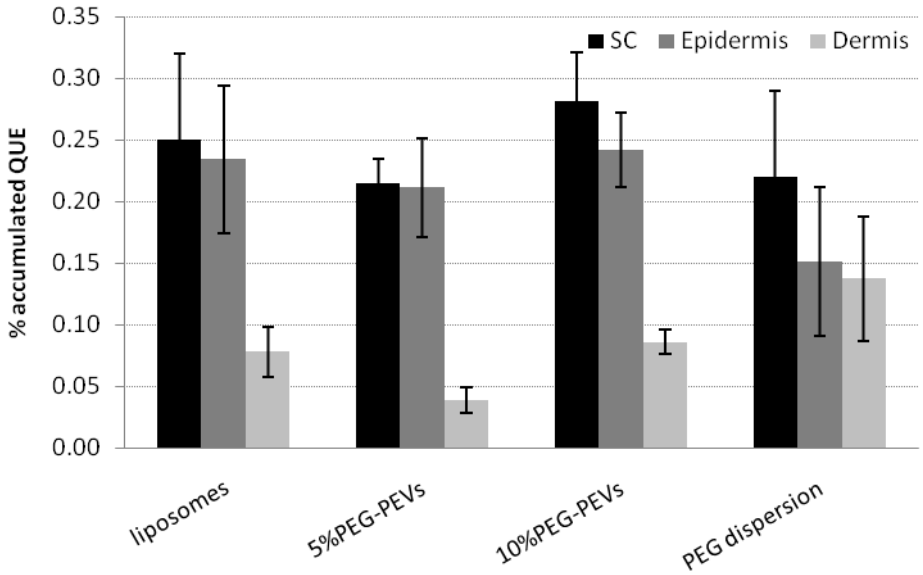

Figure 18: Cumulative amount of QUE accumulated into the stratum corneum (SC), epidermis and dermis after 24h of application of control liposomes, PEVs (5%, 10% PEG) and PEG dispersion on full-thickness mouse skin. Data represent the mean ± standard deviation of four experimental determinations.

All the studied formulation led to a transdermal QUE delivery. However, as shown in Table XXIII, also the drug delivery to the receptor medium was very low especially for conventional liposomes. The highest accumulation into the receptor fluid was obtained with 5% PEG-PEVs that were able to give a higher drug percutaneous absorption than its accumulation into the skin. All the studied formulations showed higher drug permeation into the receptor compartment than control liposomes. QUE permeation into receptor medium for 10% PEG-PEVs and PEG dispersion was similar.

Table XXIII: Total amount of QUE accumulated in the receptor medium after 24h permeation experiments through mouse skin

	Liposomes	**5%PEG-PEVs**	**10%PEG-PEVs**	**PEG dispersion**
µg /cm^2	2.61	5.08	4.82	5.66
%	0.15	0.40	0.27	0.25

Cumulative amounts of QUE diffuse through the mice skin (µg/cm^2) were calculated and plotted against time (Figure 19). It is evident that drug diffusion from PEVs and PEG dispersion was approximately 2-fold greater compared to that of liposomes. We can observe a quite linear diffusion of QUE during the first 8 hours especially with 10% PEG-PEVs.

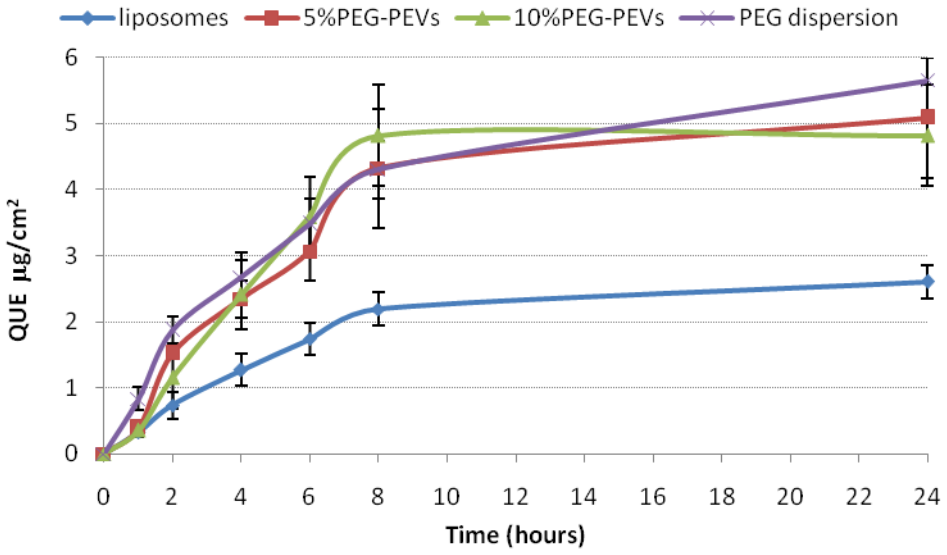

Figure 19: Permeation of QUE through mouse skin from control liposomes, 5% and 10% PEG-PEVs and PEG dispersion, determined in receptor medium of Franz diffusion cell in 24 hours. Data represent the mean ± standard deviation of four experimental determinations.

Results obtained from these experiments are not satisfying since the drug accumulation into and permeation through the skin was very low. However, it must be said that mouse skin is not the best model for *in vitro* (trans)dermal experiments and experiments through human or pig skin could give different results. In this work, the mouse skin was chosen since a further aim of the work was to test the formulations *in vivo* using mouse. Indeed, preliminary tests carried out *in vivo* have shown that the tested formulations are actually active in an inflammation model on mice.

5 Conclusion

In the present work, innovative liposomes with QUE were prepared using phosphatidylcholine and PEG, OA, or both of them. Designed OA-PEVs and PEG-OA-PEVs were obtained with suitable MD and ZP but did not show appropriate stability. Increased solubility of QUE in PBS and PEG-PBS solution was proven. The presence of PEG increased drug solubility by 3.5- and 5.1-fold with 5% and 10% PEG, respectively. Mean diameter of prepared particles increased as a function of the presence of loaded QUE and quantity of the PE. Liposomes chosen for *in vitro* transdermal study presented average size from 128 nm to 328 nm and surface charge from -6 mV to -8 mV. Cryo-TEM analysis confirmed the formations of small and fairly spherical vesicles with different lamellarity and presence of invaginated vesicles. QUE was incorporated in liposomes and PEG-PEVs with high EE% (from 52% in liposomes to 75% in 5% PEG-PEVs) and Stewart assay showed high aggregation efficiency (71-74%).

Franz diffusion vertical cells were used to evaluate accumulation into and diffusion of QUE through full thickness CD-1 mouse skin. The amount of QUE in skin layers was very low (less than 1% in total with all of the samples). No statistically significant enhancement of accumulation was demonstrated among the control liposomes, PEG-PEVs and PEG dispersion after the transdermal study ($p>0.05$). The total mean amount of QUE deposited into the skin was always higher in the SC than in epidermis and dermis. All the studied formulation led to a transdermal QUE delivery, but the drug delivery to the receptor fluid was very low. The highest accumulation into the receptor fluid was obtained with 5% PEG-PEVs that gave a higher drug percutaneous absorption than its accumulation into the skin. All the studied formulations showed higher drug permeation into the receptor compartment than liposomes. Drug diffusion through mice skin from PEVs and PEG dispersion was approximately 2-fold greater compared to that of liposomes.

Some important improvements regarding QUE dermal delivery have been achieved during the present study. QUE solubility was increased in PBS and QUE was incorporated in PEG-PEVs with high EE%. However, results obtained from *in vitro* transdermal study are not satisfying since the drug accumulation into and permeation through the skin was very low. Experiments through human or pig skin could have given different results, since mouse skin is not the best model for *in vitro* transdermal experiments.

References

1) Harborne JB, Williams CA: Advances in flavonoid research since 1992. Phytochem. 2000; 55: 481–504.
2) Di Carlo G, Mascolo N, lzzo AA, Capasso F: Flavonoids: Old and new aspects of a class of natural therapeutic drugs. Life Sciences 1999; 65 (4): 337 – 353.
3) Beecher GR: Overview of dietary flavonoids: nomenclature, occurrence and intake. J Nutr. 2003; 133 (10): 3248S-3254S.
4) Paliyath G, Bakovic M, Shetty K: Functional Foods, Nutraceuticals and Degenerative Disease Prevention http://books.google.si/books?id=bGpuyrFr9M8C&pg=RA2-PA1991&lpg=RA2-PA1991&dq=flavanonol+occurrence&source=bl&ots=pl9lcvgiht&sig=XEuRJUdO4rr_GMZmlDlHtEzMcuQ&hl=sl&sa=X&ei=FPDFUsHeHceMtAbF8IHYCQ&redir_esc=y#v=onepage&q=flavanonol%20occurrence&f=false Accessed January 4, 2014
5) Higdon, J: Flavonoids. http://lpi.oregonstate.edu/infocenter/phytochemicals/flavonoids/#tab1 Accessed June 26, 2013.
6) Hooper L, Kroon1 PA, Rimm EB, Cohn JS, Harvey I, et al: Flavonoids, flavonoid-rich foods, and cardiovascular risk: a meta-analysis of randomized controlled trials. Am J Clin Nutr 2008; 88: 38–50.
7) Ravishankar D, Rajora AM, Greco F, Osborn HMI: Flavonoids as prospective compounds for anti-cancer therapy. Int J Biochem Cell Biol (2013); 45(12): 2821-31.
8) Chen-yu G, Chun-fen Y, Qi-lu L, Qi T, Yan-wei X, Wei-na L, Guang-xi Z: Development of a quercetin-loaded nanostructured lipid carrier formulation for topical delivery. Int. J. Pharm. 2012; 430: 292–298.
9) Boots AW, Haenen GR, Bast A: Health effects of quercetin: from antioxidant to nutraceutical. Eur J Pharmacol. 2008; 585(2-3): 325-37.
10) Hollman, PC, Kata, MB: Dietary flavonoids: intake, health effects and bioavailability. Food Chem. Toxicol. 1999; 37: 937-942.
11) Morrow DM, Fitzsimmons PE, Chopra M, McGlynn H: Dietary supplementation with the anti-tumour promoter quercetin: its effects on matrix metalloproteinase gene regulation. Mutat Res 2001; 480-481: 269-276.

12) Lee YK, Hwang JT, Kwon DY, Surh YJ, Park OJ: Induction of apoptosis by quercetin is mediated through AMPKa1/ASK1/p38 pathway. Cancer Letters 2010; 292: 228–236.
13) Ferry DR, Smith A, Malkhandi J, Fyfe DW, de Takats PG, Anderson D, Baker J, Kerr DJ: Phase I clinical trial of the flavonoid quercetin: pharmacokinetics and evidence for in vivo tyrosine kinase inhibition. Clin Cancer Res. 1996; 2(4): 659-68.
14) Manjeet KR, Ghosh B: Quercetin inhibits LPS-induced nitric oxide and tumor necrosis factor-alpha production in murine macrophages. Int. J. Immunopharmacol. 1999; 21: 435-43.
15) Geraets L, Moonen HJJ, Brauers K, Wouters EFM, Bast A, Hageman GJ: Dietary flavones and flavonoles are inhibitors of poly(ADP-ribose)polymerase-1 in pulmonary epithelial cells. J. Nutr. 2007; 137: 2190-95.
16) Bureau G, Longpré F, Martinoli MG: Resveratrol and quercetin, two natural polyphenols, reduce apoptotic neuronal cell death induced by neuroinflammation. J. Neurosci. Res. 2008; 86 (2): 403-10.
17) MacNee W: Oxidative stress and lung inflammation in airway diseases. Eur. J. Pharmacol. 2001; 429: 195-207.
18) Nair MP, Mahajan S, Reynolds JL, Aalinkeel R, Nair H, Schwartz SA, Kandaswami C: The flavonoid quercetin inhibits proinflammatory cytokine (tumor necrosis factor alpha) gene expression in normal peripheral blood mononuclear cells via modulation of the NF-kappabeta system. Clin. Vaccine Immunol. 2006; 13: 319-28.
19) Sim GS, Lee BC, Cho HS, Lee JW, Kim JH, Lee DH, Kim JH, Pyo HB, Moon DC, Oh KW, Yun YP, Hong JT: Structure activity relationship of antioxidative property of flavonoids and inhibitory effect on matrix metalloproteinase activity in UVA-irradiated human dermal fibroblast. Arch. Pharm. Res. 2007; 30: 290-98.
20) Vicentini FTMC, Fonseca YM, Pitol DL, Iyomasa MM, Bentley MVLB, Fonseca MJV: Evaluation of Protective Effect of a Water-In-Oil Microemulsion Incorporating Quercetin Against UVB-Induced Damage in Hairless Mice Skin J Pharm Pharmaceut Sci 2010; 13(2): 274-85.
21) Weng Z, Zhang B, Asadi S, Sismanopoulos N, Butcher A, Fu X, Katsarou-Katsari A, Antoniou C, Theoharides TC: Quercetin is more effective than cromolyn in blocking human mast cell cytokine release and inhibits contact dermatitis and photosensitivity in humans. PloS One 2012; 7: e38802.

22) Lin CF, Leu YL, Al-Suwayeh SA, Ku, MC, Hwang TL, Fang JY: Anti-inflammatory activity and percutaneous absorption of quercetin and its polymethoxylated compound and glycosides: the relationships to chemical structures. Eur. J. Pharm. Sci. 2012; 47: 857-64.
23) Silva ID, Gaspar J, da Costa GG, Rodrigues AS, Laires A, Rueff J: Chemical features of flavonols affecting their genotoxicity. Potential implications in their use as therapeutical agents. Chem. Biol. Interact. 2000; 124: 29–51.
24) Li HL, Zhao XB, Ma YK, Zhai GX, Li LB, Lou HX: Enhancement of gastrointestinal absorption of quercetin by solid lipid nanoparticles. J. Control. Release 2009; 133: 238-44.
25) Gugler R, Leschik M, Dengler HJ: Disposition of quercetin in man after single oral and intravenous doses. Eur. J. Clin. Pharm. 1975; 9: 229-34.
26) Rothwell JA, Day AJ, Morgan MR: Experimental determination of octanol–water partition coefficients of quercetin and related flavonoids. J. Agric. Food Chem. 2005; 53: 4355-60.
27) Bonina F, Lanza M, Montenegro L, Puglisi C, Tomaino A, Trombetta D, Castelli F, Saija A: Flavonoids as potential protective agents against photo-oxidative skin damage. Int. J. Pharm. 1996; 145: 87–94.
28) Sinico C, Fadda AM: Vesicular carriers for dermal drug delivery. Expert Opinion on Drug Delivery 2009; 6(8): 813-25.
29) Roberts MS: Targeted drug delivery to the skin and deeper tissues: role of physiology, solute structure and disease. Clin Exp Pharmacol Physiol 1997; 24(11): 874-9.
30) Pathan IB, Setty CM: Chemical Penetration Enhancers for Transdermal Drug Delivery Systems. http://www.ajol.info/index.php/tjpr/article/download/44527/28031 Accessed August 19, 2013.
31) Chopda G: Transdermal drug delivery systems: A review. http://www.pharmainfo.net/reviews/transdermal-drug-delivery-systems-review Accessed August 19, 2013.
32) Sharma A, Saini S, Rana AC. Transdermal Drug Delivery System: A Review. http://www.ijrpbsonline.com/files/47-4184.pdf Accessed August 19, 2013.
33) Kristl J: Koža – zgradba in dogajanja v njej. http://studentski.net/gradiva/ulj/ffa/kz1/kozmeticni-izdelki-1.html Accessed August 19, 2013.

34) Elias PM. Epidermal lipids, barrier function and desquamation. J Invest Dermatol 1983; 80: 44-9.
35) Barry BW: Novel mechanisms and devices to enable successful transdermal drug delivery. J Pharm Sci. 2001; 14: 101-14.
36) Sinha VR, Kaur MP: Permeation Enhancers for Transdermal Drug Delivery. Drug Dev Ind Pharm 2000; 26(11), 1131-40.
37) Menon GK, Bommannan DB, Elias PM: High-frequency sonophoresis: permeation pathways and structural basis for enhanced permeation. Skin Pharmacol. 1994; 7: 130–139.
38) Bronaugh RL, Maibach HI: Percutaneous Absorption; Mechanisms, Methodology, Drug Delivery, 2nd Edition. Marcel Dekker, New York and Basel, 1989: 77–93.
39) Martins S, Sarmento B, Ferreira DC, Souto EB: Lipid-based colloidal carriers for peptide and protein delivery – liposomes versus lipid nanoparticles. Int J Nanomedicine 2007; 2(4): 595-607.
40) Senior JH: Fate and behavior of liposomes in vivo: a review of controlling factors. Crit Rev Ther Drug Carrier Syst 1987; 3(2): 123-93.
41) Cadena PG, Pereira MA, Cordeiro RB, Cavalcanti IM, Barros Neto B, Pimentel Mdo C, Lima Filho JL, Silva VL, Santos-Magalhães NS: Nanoencapsulation of quercetin and resveratrol into elastic liposomes. Biochim Biophys Acta. 2013; 1828 (2): 309-16.
42) HSDB, Hazardous Substances Data Bank. Quercetin. http://toxnet.nlm.nih.gov/cgi-bin/sis/search/r?dbs+hsdb:@term+@rn+@rel+117-39-5 Accessed November 11, 2013